To the Graduate Council:

I am submitting herewith a thesis written by James R. Brewster entitled "Some Applications of Caustic Foci to Non-Destructive Evaluation." I have examined the final copy of this thesis for form and content and recommend that it be accepted in partial fulfillment of the requirements for the degree of Master of Science, with a major in Materials Science and Engineering.

K H G Ashbee

Kenneth H. G. Ashbee, Major Professor

We have read this thesis
and recommend its acceptance:

Charlie R. Brooks

David C Jaye

Accepted for the council:

C W Mintel

Vice Provost
and Dean of The Graduate School

STATEMENT OF PERMISSION TO USE

In presenting this thesis in partial fulfillment of the requirements for a master's degree at the university of Tennessee, Knoxville, I agree that the library will make it available to borrowers under the rules of the library. Brief quotations from this thesis are allowable without special permission, provided that accurate acknowledgment of the source is made.

Permission for extensive quotation from or reproduction of this thesis may be granted by my major professor, or in his absence, by the head of Interlibrary Services when, in the opinion of either, the proposed use of the material is for scholarly purposes. Any copying or use of this material for financial gain shall not be allowed without my written permission.

Signature James Brost

Date April 21st 1989

SOME APPLICATIONS OF CAUSTIC FOCI TO NON-DESTRUCTIVE EVALUATION

A Thesis

Presented for the

Master of Science

Degree

The University of Tennessee, Knoxville

James R. Brewster

May 1989

ACKNOWLEDGMENTS

I wish to thank all those without who the work presented here would not of been possible:

Mike Rogers, Doug Fielding and Ron Johnson for building and maintaining my equipment so well.

Dr. Ken Ashbee for giving me the opportunity to study in America and for encouraging my personal research interests.

Professor J. F. Nye whose enlightening discussions are the origin of my interest in caustics.

And, of course, my laboratory colleges; Dr David Tossel, Zheng Rong Xu and Steve Joslin for acting as sounding boards for my ideas and providing many helpful suggestions.

ABSTRACT

The application of caustic foci to non-destructive evaluation (N.D.E.) yields novel testing techniques with advantages over conventional methods.

In situations where the wavelength is relatively small, any wave field can be approximated by a families of rays drawn along the direction of energy flow. Caustics are the envelopes of such rays representing surfaces of high intensity, which implies that they give a general representation of the focusing of the waves. The usefulness of caustics in N.D.E. stems from the fact that they constitute well defined geometric entities inside the test specimen with which to probe its internal structure.

The research presented here involves the application of caustics to the ultrasonic testing of rods or pipes and acoustic or optical imaging.

The location of small defects inside rods using the caustics formed by the sound scattered from them has been demonstrated. Techniques for locating the ends of extended cracks, both internal and surface-breaking, are also presented.

The caustic formed by sound reflected from a cylindrical dish has been used to image both the internal structure and the surfaces of materials.

The theory behind a high depth of field optical microscope utilizing caustics is given.

TABLE OF CONTENTS

CHAPTER	PAGE
1. INTRODUCTION	1
2. THE FUNDAMENTALS OF ULTRASOUND	10
3. LITERATURE REVIEW	17
4. CALCULATIONS AND COMPUTER PROGRAMS USED	19
5. APPARATUS USED	21
6. THE CAUSTICS FORMED BY SOUND SCATTERED FROM DEFECTS	26
Theory	26
Experimental	31
Results	35
Discussion	38
Conclusion	42
7. CAUSTICS AND THE SIZING OF EXTENDED DEFECTS	43
Theory	43
Experimental	46
Results	48
Discussion	51
Conclusion	53
8. CAUSTICS AND THE SHADOWS OF SURFACE BREAKING DEFECTS	54
Theory	54
Experimental	59
Results	61
Discussion	68
Conclusion	70

9. ULTRASONIC IMAGING UTILIZING CAUSTICS 71

Theory 71

Experimental 74

Results 77

Discussion 81

Conclusion 85

10. A HIGH DEPTH OF FIELD OPTICAL MICROSCOPE 86

Theory 86

11. DISCUSSION OF APPLICATIONS TO N.D.E. 92

12. CONCLUSIONS AND SUGGESTED FUTURE RESEARCH 100

LIST OF REFERENCES 102

APPENDIXES 105

APPENDIX A. CALCULATION OF THE ORIENTATION OF THE CAUSTIC AT INFINITY 106

APPENDIX B. THE LOCUS OF THE CAUSTIC FORMED BY A CIRCULAR REFLECTOR 110

VITA 113

LIST OF FIGURES

FIGURE		PAGE
1.1.	A Simple Two-Dimensional Caustic	2
1.2.	The Caustic Formed by a Coffee Cup	2
1.3.	A Diagram of the Rays Responsible for the Formation of the Rainbow	4
1.4.	Sound Waves From a Point Source Diverging on Being Refracted by the Sample Wall	6
1.5.	Caustic Formed by Rays Reflected From the Sample Wall	6
1.6.	Defect Crossing Caustic as Sample is Rotated	7
2.1.	Sound Ray Incident on a Plane Boundary Between Two media	13
5.1.	The Experimental Test Rig	22
5.2.	A Plan View of the Rig	22
5.3.	Plan View of the Rig Set Up to Image a Sample	23
6.1.	A Point Source of Shear Waves Inside an Aluminum Cylinder	27
6.2.	Sound Reflected From the Inner Wall	27
6.3.	Caustic Formed After Refraction into the Surrounding Water	28
6.4.	The Principle of Reciprocity as it Applies to These Caustics	30
6.5.	A Nearly Straight Caustic	30
6.6.	Schematic Diagram of Test Setup	32
6.7.	The Amplitudes of the Received Signals	36
6.8.	The Times of Arrival of the Received Signals	36
6.9.	The Ray Paths Present	37
6.10.	The Intensity Profile Across the Caustic	37

6.11. The Separation of the Caustics as a Function of Defect Position 39

6.12. Comparison of results with Airy Theory for Shear 39

6.13. Comparison of results with Airy Theory for Compression 40

7.1. Crack Entirely Inside Shadow Zone 45

7.2. Caustic Incident on Crack 45

7.3. The Ray Path of the Received Signal 49

7.4. Variation of Signal Starting Point with Sample Orientation 49

7.5. Variation of Signal Starting Point with Sample Orientation 50

7.6. Construction of the Caustics Touching the Crack Tip ... 52

7.7. The Level of Uncertainty Involved 52

8.1. Three Possible Crack Locations 55

8.2. Diffraction at an Edge 55

8.3. Rays Refracted Out After Forming Internal Caustic 57

8.4. Schematic Test Configuration 57

8.5. The Three Different Situations to be Considered as the Crack Tip Crosses the Caustic 58

8.6. Amplitude Profile with Probes 145 Degrees Apart 62

8.7. Amplitude Profile with Probes 180 Degrees Apart 62

8.8. Amplitude Profile with Probes 210 Degrees Apart 63

8.9. The Amplitude Profiles For 3 Receiver Positions 65

8.10. Amplitude Profiles Relative to Receiver 65

8.11. System Configuration Diagram --Shorter Slot 67

8.12. System Configuration Diagram --Longer Slot 67

9.1. Caustic Formed by Rays Reflected From Dish 72

9.2. Schematic Test Setup 72

9.3. Computer Generated Image of a Right Angled Corner 78

9.4. Computer Generated Image of an Aluminum Honeycomb 80

9.5. An Aluminum Honeycomb 80

9.6. Computer Generated Image of a Wooden Surface 82

9.7. A Wooden Fracture Surface 82

9.8. Computer Generated Image of a Metallic Fracture Surface 83

9.9. A Metallic Fracture Surface 83

10.1. The Optical Caustic Formed by a Cylindrical Mirror 87

10.2. Schematic Diagram of the Microscope 87

10.3. Plan View of the Specimen 88

11.1. The Fraction of the Pipe Thickness Hidden as a Function of its Geometry 95

A-1. The Ray Path of the Sound Scattered From a Defect at S 107

B-1. Ray Reflected by a Circular Reflector 111

CHAPTER 1

INTRODUCTION

Caustics are the most general way of describing the focusing of a wavefield. They are surfaces of high wave intensity as opposed to the point focus of paraxial optics.

In situations where the wavelength is small compared to the physical dimensions of the problem, any wavefield can be approximated by bundles of rays drawn along the direction of wave propagation. In this case a caustic is the envelope of these rays, that is, a surface to which all rays are tangential. This is most easily illustrated using the 2-dimensional case in which caustics are lines (figure 1.1). As ray models are usually formulated such that the intensity of radiation is proportional to the density of rays, it is evident from figure 1.1 that energy is highly concentrated near the caustic. In fact it can be shown that the density of rays is infinite on the caustic, implying that a more accurate model of the wavefield is required near these singularities. It can also be observed that a caustic forms a well defined boundary to a set of rays; on crossing a caustic one moves from a region of shadow into one of illumination by rays. This is still true when the effect of finite wavelength is included, but with a more gradual transition between illumination and shadow.

Figure 1.2 depicts perhaps the most familiar example of a caustic; the cusped curve formed on your drink when a coffee cup

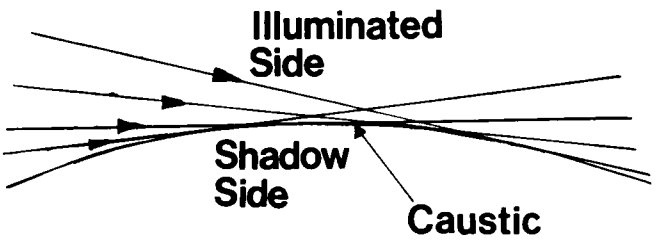


Figure 1.1. A Simple Two-Dimensional Caustic

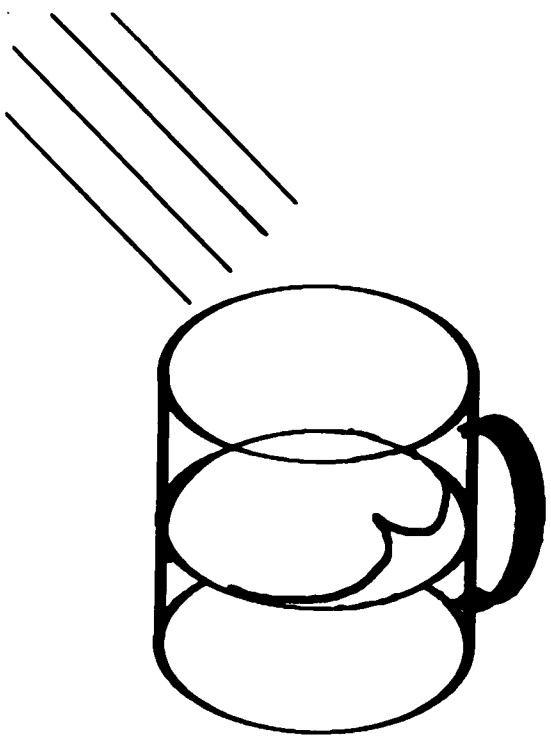


Figure 1.2. The Caustic Formed by a Coffee Cup

is illuminated by a distant (or small) light source. The observed curve is the intersection of the liquid surface and the caustic surface which runs parallel to the axis of the cup. The same focusing geometry will be utilized in some of the ultrasonic experiments presented below. Another less obvious, but more spectacular, phenomenon due to the formation of caustics is the rainbow. When rays of light from the sun are reflected on the inside of a raindrop they form a caustic that tends to a straight line at infinity (see figure 1.3). In 3-dimensions this line is rotated into a cone, and those raindrops for which this cone subtends to the observer appear the brightest in the sky, thus forming the arc of the rainbow.

Non-destructive evaluation (N.D.E), that is methods by which one can assess a test object without altering its properties, is a large and very important engineering discipline. In many applications the ability to detect and/or size defects is the limiting factor in the design and safe operation of an engineered system. An example of this is the aircraft industry where airlines must balance the risk of accidents against the cost and time taken by their N.D.E operations. Many technologies have been applied to N.D.E.; almost the whole spectrum of electromagnetic radiation from X-ray through infrared to microwave, acoustic emission, eddy current induction and ultrasound have all been utilized to probe objects for defects [THOMPSON 1988]. A good overview of ultrasonic testing is given by Krautkramer [KRAUTKRAMER and KRAUTKRAMER 1983].

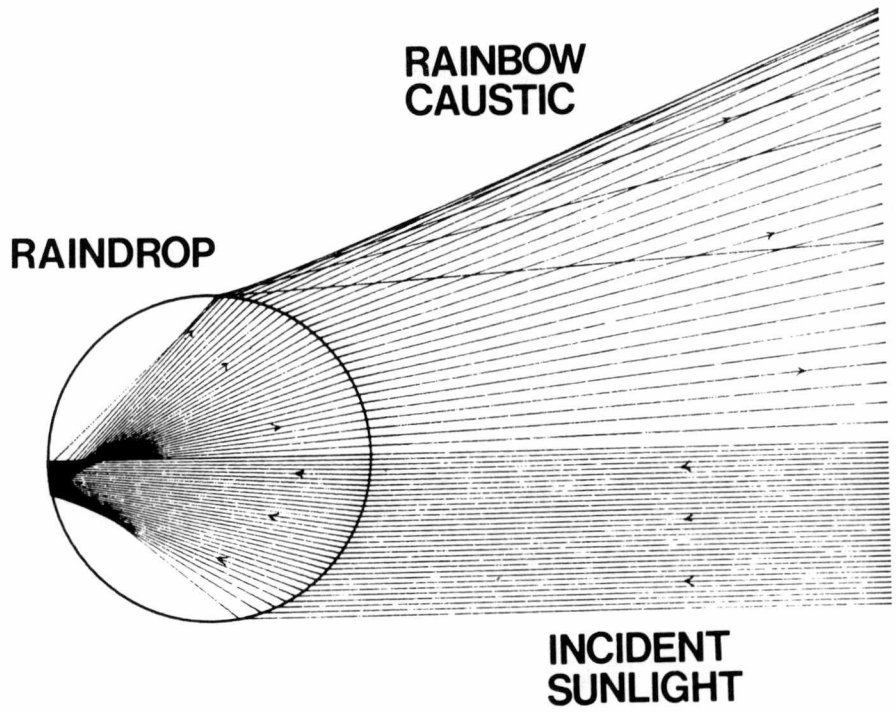


Figure 1.3. A Diagram of the Rays Responsible for the Formation of the Rainbow

The potential usefulness of caustics in N.D.E arises from the fact that a caustic constitutes a known geometric object either inside or in the medium surrounding the specimen under test. The two properties of a caustic, high intensity and sharp transition between illumination and shadow, can both be exploited. The use of caustics in N.D.E is best illustrated by giving an example of an ultrasonic method for the inspection of cylindrical objects utilizing one.

Consider an aluminum rod immersed in water and illuminated by an ultrasonic transducer. Figure 1.4 shows a transverse cross-section of the beam of compression waves leaving the source (which initially can be assumed to be point-like) being mode-converted and refracted on contact with the rod to form a sharply diverging beam of shear waves inside the sample. If the sound rays are now reflected off the inner wall, remaining in shear mode, they will form the cusped caustic shown in figure 1.5.

Consider the ultrasonic transducer being used in pulse/echo mode with the reflected signals displayed as a function of time on an oscilloscope. Suppose the rod contains a small void. Rotation of the sample will cause this defect to move along the circular path shown on figure 1.6, crossing the caustic at the point X. If the rod is now rotated so that the defect moves from the shadow side of the caustic to the illuminated zone, a new echo will appear on the oscilloscope screen as the defect crosses the caustic. This echo will be strong due to the focusing effect.

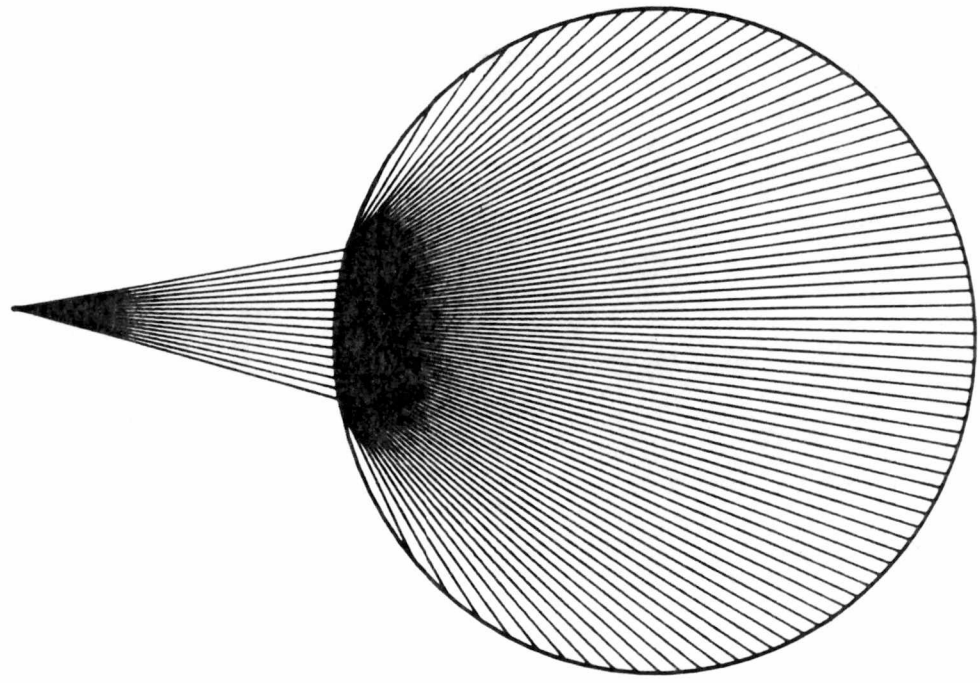


Figure 1.4. Sound Waves From a Point Source Diverging on Being Refracted by the Sample Wall

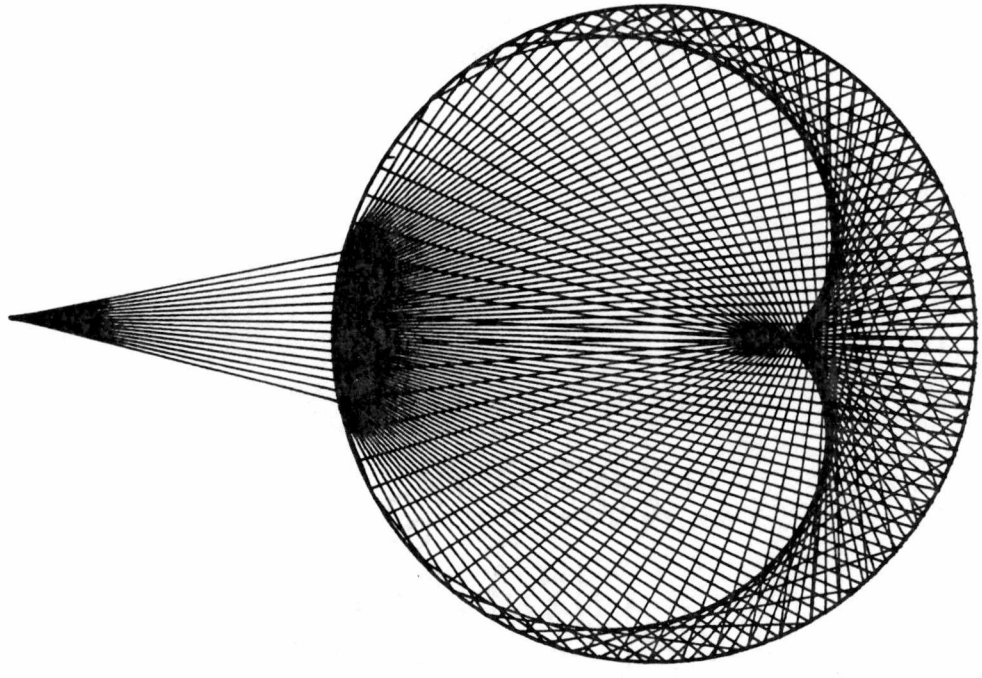


Figure 1.5. Caustic Formed by Rays Reflected From the Sample wall

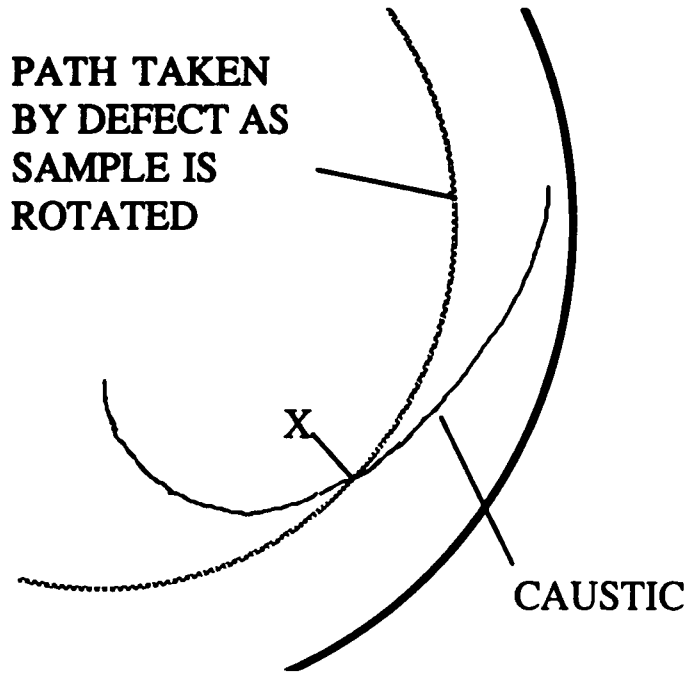


Figure 1.6. Defect Crossing Caustic as Sample is Rotated

As mentioned above the ray approximation breaks down on the caustic necessitating that the effects of finite wavelength be taken into account in the vicinity of the caustic. The wave field around a caustic was solved in the nineteenth century by G.B. Airy [AIRY 1838]. Because their locus is geometrically related to that of the caustic, this diffraction problem can be solved by the direct application of Huygens' principle to the wavefronts in the vicinity of the caustic. This bypasses the approximations implicit in Fresnel and Fraunhofer diffraction theory [LANDAU and LIFSHITZ 1951].

The result Airy derived is:

$$I(x)=A\left[\frac{2k^2}{\rho}\right]^{1/6}\times\Phi\left[x\cdot\left[\frac{2k^2}{\rho}\right]^{1/3}\right] \tag{1.1}$$

Where I is the intensity of radiation as a function of the distance from the caustic x (defined so that points on the shadow side have positive x), ρ is the radius of curvature of the caustic, k is the wavenumber and $\Phi(t)$ is the Airy function defined by:

$$\Phi(t)=\frac{1}{\sqrt{\pi}}\int_0^{\infty}\cos\left[\frac{\zeta^3}{3}+\zeta t\right]d\zeta \tag{1.2}$$

This integral appears in several other mathematical contexts has been extensively studied and tabulated in handbooks [ABRAMOWITZ and STEGUN 1964].

The Airy function has its first and largest maximum at t=-1.02, implying that the intensity is greatest at a distance

inside the illuminated zone given by:

$$x_{max} = -1.02 \times \left[\frac{\rho}{2k^2}\right]^{1/3} \qquad (1.3)$$

Actually on the caustic the intensity is predicted to be about 36% of this value, therefore x_{max} can be taken to be a measure of the width of the caustic. Note that the caustic becomes broader as ρ is increased but only as its cube root; a thousand-fold increase in the radius of curvature results in a caustic of only ten times the width.

The purpose of the research presented in this thesis is to explore the possible application of ultrasonic caustics to N.D.E. in order to assess the advantages and drawbacks of these techniques. Three novel testing techniques, relevant to three broad classes of defects, have been examined. In addition, a method of ultrasonic imaging and the theory behind a design of high depth of field optical microscope involving caustics are presented.

CHAPTER 2

THE FUNDAMENTALS OF ULTRASOUND

In order to aid the reader in understanding the research and theory presented in this thesis this chapter gives an outline of the relevant aspects of acoustics. Some knowledge of general wave theory has been assumed.

Sound waves are travelling waves of stress and strain and ultrasound is defined to be any sound of too high a frequency to be detected by the human ear. Typical ultrasonic applications require frequencies in the megahertz (MHz) range, about one hundred times higher than the upper frequency limit of the ear.

Inside a solid there are two possible modes of propagation of sound, shear waves and compression waves. In a shear wave the displacement of the particles in the medium is normal to the direction of propagation of the wave, implying that the stress field associated with the wave is one of pure shear stress. Alternatively, in a compression wave the material particles are displaced along the direction of propagation creating a field of compressive stress. A general disturbance can always be expressed in terms of a sum of shear and compression components of various frequencies, phases and directions. As a result of the fact that compression waves always travel faster than shear waves, the two modes will separate from each other once they start to propagate. Because they can not support a shear stress, only compression

waves are found in fluids. Any process that changes one mode of sound to another is referred to as mode-conversion.

Surface waves exist on the boundaries between materials and there are also modes of propagation unique to rods and plates that are thin on the scale of the wavelength.

In most metals sound exhibits very little dispersion, that is, the velocity of propagation is independent of frequency and amplitude. This is important to ultrasonic N.D.E. because it implies that a pulse of sound is propagated in bulk material without distortion.

The attenuation of sound by the medium in which it travels can be attributed to two mechanisms; absorption, the dissipation of the sound wave's energy as heat and scattering, the disruption of the wave due to the inhomogeneity and/or anisotropy of the material. The former is present in all media its effect rapidly increasing with frequency [MASON 1968]. Absorption of sound by water limits any long range immersion testing technique to frequencies less than about 20 MHz. Scattering of sound by the anisotropic grains is the chief source of attenuation in a polycrystalline metal. This effect increases as the cube of the frequency and becomes important as the wave length approaches about ten times the average grain size [KRAUTKRAMER and KRAUTKRAMER 1983]. Attenuation thus imposes a lower limit of about 0.25 mm on the wavelength and, therefore, an upper frequency limit on the order of 10 MHz on the ultrasonic testing of typical

metals.

If a sound wave, that can be approximated by a set of rays, encounters a smooth (on the scale of the wavelength) boundary between two materials, reflection, refraction and mode-conversion will occur. In general one incident sound ray will produce two reflected rays, two rays refracted into the second medium and surface waves (figure 2.1).

All refractions and reflections obey Snell's law in its most general form:

$$\frac{\sin\theta_i}{\sin\theta_r} = \frac{\text{velocity of incident sound wave}}{\text{velocity of refracted/reflected soundwave}} \qquad (2.1)$$

Where θ_i and θ_r are angles of incidence and refraction/reflection defined as indicated in figure 2.1. If there is no mode-conversion the angle of reflection is equal to the angle of incidence.

Ultrasound is usually generated by electrically exciting a piezoelectric crystal. An ultrasonic probe consists of a transducer crystal mounted in a casing designed to best fit the application involved. Some probes, for example, are designed to be used to produce compression waves in free water whilst others are placed on the surface of the sample generating shear waves inside. (In this thesis the terms "transducer" and "probe" will be used interchangeably; strictly, the transducer is the piezoelectric crystal and the probe is the combination of the transducer and its mounting.)

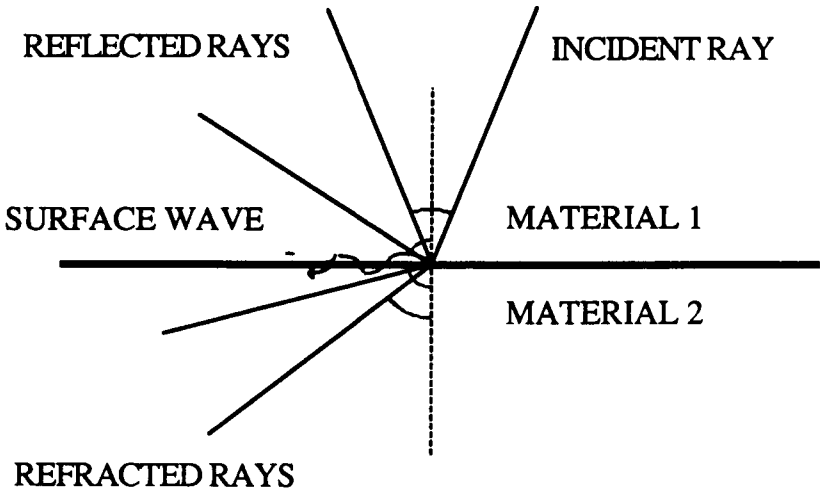


Figure 2.1. Sound Ray Incident on a Plane Boundary Between Two Media

A pulse of sound is produced by applying a sharp spike of voltage to the transducer causing it to vibrate around its natural resonant frequency. These vibrations are damped in a controlled way by a variable electrical resistance in parallel with the transducer. Adjusting this resistance allows control of the pulse length. Continuous sound radiation is produced by stimulating the transducer with an oscillating voltage tuned to the resonant frequency of the crystal. Ultrasonic transducers also receive sound waves, converting them to radio-frequency electrical signals.

To interpret the received signals it is important to understand the nature of the sound field produced by a transducer. A flat faced transducer, as used in all experiments presented in this thesis, can be modeled quite well by assuming that the whole transducer face vibrates in unison akin to an oscillating piston. In this case the transducer face is equivalent to an aperture in an opaque screen illuminated from behind by a coherent source of plane waves. This allows the application of standard Fresnel and Fraunhofer diffraction theory [BORN and WOLF 1964]. The most important result of this is that the sound field is divided into two regions; the near field, where interference effects are strong and the far field, where the amplitude of the beam is more slowly varying. For a circular aperture the near field extends a distance N from the probe given by:

$$N \simeq \frac{D^2 - \lambda^2}{4\lambda} \qquad (2.2)$$

Where, D is the diameter of the transducer face and λ is the wavelength [KRAUTKRAMER and KRAUTKRAMER 1983].

In the far field the beam diverges at an angle γ given by:

$$\sin\gamma \approx 1.2 \cdot \frac{\lambda}{D} \qquad (2.3)$$

The value of ultrasonic vibrations in non-destructive evaluation stems from the relative ease with which they travel through solid material. Defects in a material manifest themselves by reflecting sound waves allowing either an echo or a shadow behind the flaw to be detected.

A pulse-echo test involves producing a pulse of sound and observing the returning echo signals. One transducer often performs as both transmitter and receiver, but in some cases the ray geometry dictates that two separate probes be used. In order to gain information about defect location and size, the transducer is scanned and the variation of the echoes with probe position studied. The ways in which the data can be handled fall into three broad categories:

1. "A-scan", the amplitudes of the incoming signals are displayed as a function of time at a fixed transducer location.

2. "B-scan", the time of arrival of the echo signals are plotted as a function of one probe coordinate.

3. "C-scan", the amplitude of the echo signal is plotted as a function of two probe coordinates.

The C-scan requires shading or coloring of the data according to signal strength which is also done to augment many modern

B-scan systems.

Scanning a probe over an object is equivalent to creating a large synthetic aperture through which the object is viewed. This allows construction of an image and sophisticated algorithms and computer hardware exist to perform this task.

Because of its relative simplicity the A-scan is widely used in industrial applications.

CHAPTER 3

LITERATURE REVIEW

There is nothing new about the concept of a caustic; the rainbow was elucidated by René Descartes in 1637 [DESCARTES 1637] and A.A.Cayley wrote a very thorough memoir about the caustics formed by circular objects in 1857 [CAYLEY 1857]. The important calculation outlined in chapter 1 was performed by G. B. Airy as early as 1838 [AIRY 1838].

Since the early nineteen seventies theoretical physicists have become more interested in the focusing of rays. This is because it has been found that the rigorous mathematical treatment of sudden changes, catastrophe theory, can be used to classify and place topological constraints on the forms of caustics [BERRY and UPSTILL 1980]. None of this deep mathematics is required for this work because the geometries involved are relatively simple and can be treated by more conventional means.

There are two previous instances of the application of ultrasonic caustics to N.D.E.. Research on the possibility of applying the caustic geometry, as presented in the introductory section, to ultrasonic N.D.E. was done by Mehram Moshfehgi and formed a chapter of his Ph.D. thesis. These experiments were published in "Ultrasonics" [MOSHFEHGI 1986]. Using rods and pipes containing both artificial and real defects, he showed that an intense new echo is observed as a defect crosses the caustic line

and was able to relate the position at which this occurred to computer drawn ray diagrams. This was to be used to complement the tomographical imaging system that he had developed [MOSHFEHGI and HANDSTEAD 1985]. He also suggested that there could be medical applications if an ultrasonic caustic could be formed within the human body. A method by which this may be done is outlined in chapter 11.

The other set of research on the exploitation of ultrasonic caustics in N.D.E. is by P. A. Doyle [DOYLE 1980]. His idea is that the diffraction of a beam of sound by a crack will form caustics behind it and within what the ray approximation would predict to be its shadow. He applied the geometrical theory of diffraction [KELLER 1956], which allows the field near a shadow to be treated in terms of rays, to predict the form of these caustics. This is a fundamentally different approach to that proposed here; caustics formed by the defect are studied rather than a known caustic being used to probe for defects.

CHAPTER 4

CALCULATIONS AND COMPUTER PROGRAMS USED

Calculations concerning the geometry of caustics were done either by ray tracing or analytically. All computer programs were written in BASIC and executed on an I.B.M. personal computer.

The ray diagrams presented were generated by a program which, given the source and direction of each ray calculates its first point of contact with an interface at which it calculates its change in direction either due to reflection of refraction. This is repeated until the ray path of interest has been traced out. The caustics are visible as the envelopes of several such rays.

This ray tracing program was adapted to measure the radii of curvature of caustics, as is required to calculate the width of the Airy diffraction peak. Points on the caustic were found by calculating the meeting points of neighboring rays. The curvature could then be measured by calculating the distance to the point equidistant to each set of three points on the caustic.

An implicit equation relating the orientation of the caustics formed at infinity by sound emanating from a point source inside a cylinder (see chapter 6) to the radial position of this source is derived in appendix 1. A computer program was written that used this expression to calculate the location of the caustics at a finite distance from the axis given the radial position of the defect responsible. This was done by assuming that the caustic is

a straight line from infinity to the finite radial location of the receiver. By comparing the results of this to those calculated exactly, by ray tracing, this approximation was found to lead to an error of only 0.1 degrees in the caustic location (for the water immersed aluminum rods used in the most of the research presented).

For the case of a circular reflector the locus of the caustic could be solved exactly throughout its length as is presented in appendix 2. The equation thus derived formed the basis for the computer program that produced the data utilized by the image construction software needed for the work described in chapter 9.

This program converted amplitude and time of flight information into an image by reading into an array a disk data file containing the coordinates of points on the caustic as a function of the time of arrival of sound at that point. This data file was created beforehand by another program which used the ray path calculation of appendix 2 to calculate the relevant point on the caustic for many, equally spaced, times of flight. Once this data was read into an array all the image construction program had to do was to take the signal time of flight and calculate the subscript of the row containing the coordinates of the point from which theechoes originated. This BASIC program could read data off the disk and calculate image points at a rate of 6 per second. The rate of operation could be increased many fold by writing the program in a low level language and using a faster computer.

CHAPTER 5

APPARATUS USED

The apparatus consisted of an immersion testing rig and ultrasonic transducers connected to electronics capable of producing and receiving ultrasonic signals. Figures 5.1 and 5.2 show the rig set up to test a sample using two probes. Figure 5.3 is a plan view of the rig set up to image an aluminum honeycomb as described in chapter 9. All experiments were conducted in a 75 cm by 60 cm stainless steel tank with the rig fully immersed in water.

The rig was constructed mainly of brass and designed to mount the cylindrical samples and to allow an ultrasonic transducer to be moved on a circular track concentric with the sample axis. Another probe could be mounted at a fixed position in front of the sample. The sample could be rotated and its angular position and the position of the movable probe could be measured. Angular measurement was made possible by radial markers scored onto the base of the rig at five degree intervals.

Samples were attached to the rig by screwing them onto a central, cylindrical sample holder. The sample holder was attached to the base of the rig by fitting over a sleeve projecting up from it. The orientation of the sample could be locked by hand tightening a screw pressing on to the base. The position of the sample could be measured by recording the position of a pointer

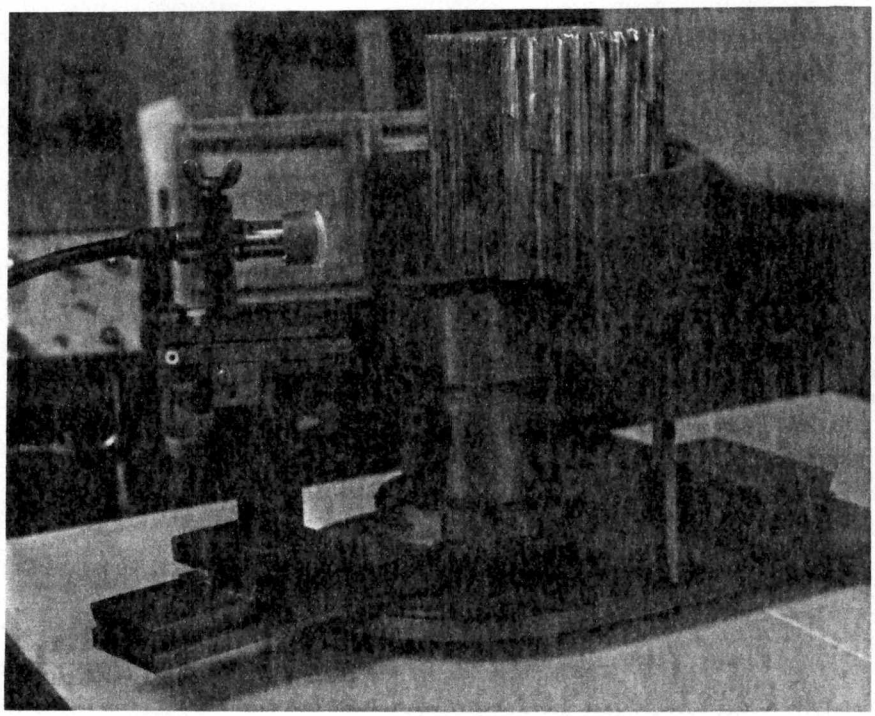


Figure 5.1. The Experimental Test Rig

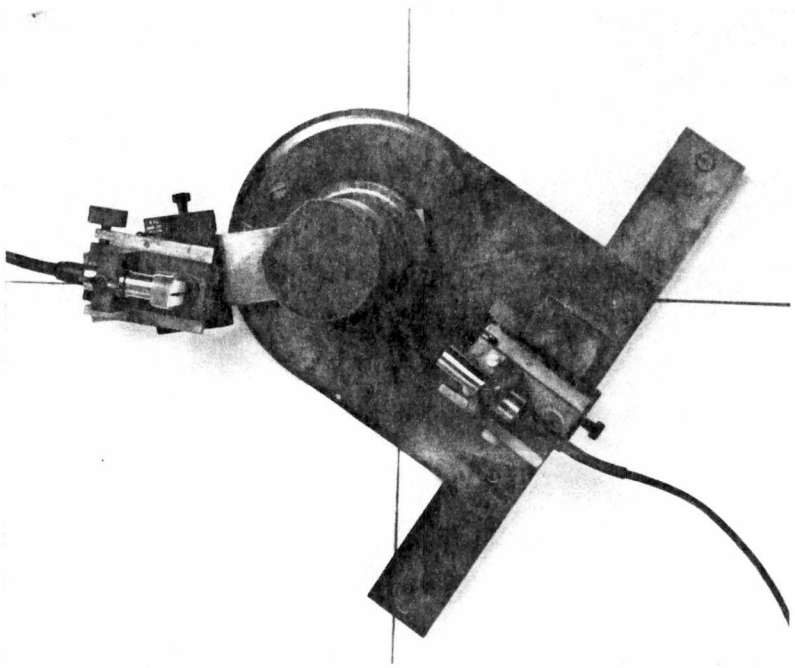


Figure 5.2. A Plan View of the Rig

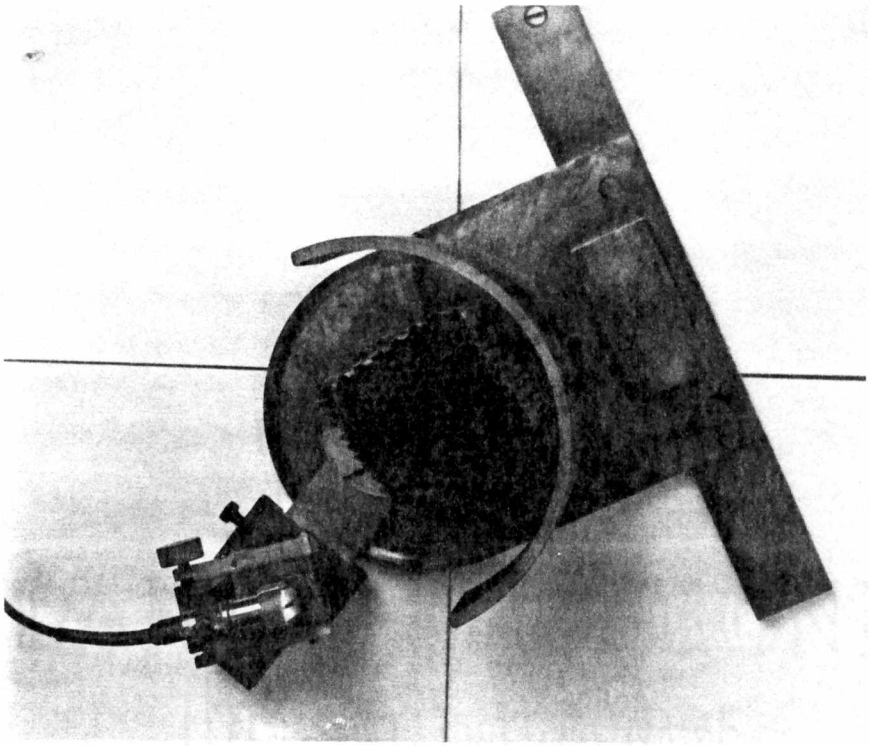


Figure 5.3. Plan View of the Rig Set Up to Image a Sample

attached to the sample holder against the scale scored onto the base.

Both transducer holders were mounted on rails, designed to be compatible with the standard optical bench manufactured by Oriel Corporation. The movable rail had a hole machined into it through which passed a member attached to the base. This allowed the rail to be rotated about the sample axis. More precise measurement of the angular position of this probe was made possible by a ten degree section of a transparent plastic protractor attached to the rail through which the scale scored onto the base could be seen.

Probe holders were designed so that the probes could be rotated in the horizontal plane about an axis passing through the transducer face. This was done by hand turning a screw; the desired degree of offset was achieved by counting the number of turns.

The probe holders were connected to rods mounted onto the rails via Oriel optical table vertical rod holders. This allowed smooth translation of the probes along the rails.

The ultrasonic transducers were manufactured by Panametrics. The 5 MHz transducers were of type "V309" with a flat, circular face of diameter 12.5 mm, and 20 MHz transducers with a similar face 7mm in diameter, type "V317".

These were used with a Panametrics pulser/receiver, model "5052PR". This stimulated the transducers with a short high voltage signal then amplified the received signals sending its

output to an oscilloscope. It had two modes of operation; pulse-echo mode, transmitting and receiving signals from the same transducer and pitch-catch mode, stimulating one transducer and then receiving signals from an other. The pulser/receiver sent a triggering signal to the oscilloscope coincident with the production of the sound pulse. The pulse rate, on the order of a kilohertz, and the damping of the transducer could be continuously varied.

The signals were displayed on a Tektronix, 100 MHz oscilloscope, model "2236". This was triggered by the pulser/receiver and had the capability to magnify a window of the time scan and to measure the time of arrival of signals, relative to the initial trigger, to about the nearest 0.05 μs.

CHAPTER 6

THE CAUSTICS FORMED BY SOUND SCATTERED FROM DEFECTS

As well as caustics being formed inside a cylindrical object by incident sound, they are also produced by sound scattered from an internal defect. A knowledge of both cases and the relationship between them is useful in understanding their application to N.D.E..

Theory

Consider a point source of shear mode sound inside a water immersed Aluminum rod (figure 6.1). If this spherical wave is now reflected off of the inner wall of the specimen, remaining in shear mode, a triple cusped caustic is formed inside the cylinder as shown by the ray diagram figure 6.2. If these rays are now refracted out into the surrounding water the caustic formed is a pair of very slightly curved lines which tend to an asymptotic direction at infinity (figure 6.3). This caustic is similar to that which causes the rainbow, the difference being that the object responsible has cylindrical symmetry, so that in three dimensions the caustic is a pair of planes parallel to the cylinder axis rather than a cone.

The rays of figure 6.3 are not independent from those shown in figure 1.5; they are related by a general property of solutions to the wave equation, the principle of reciprocity [RAYLEIGH

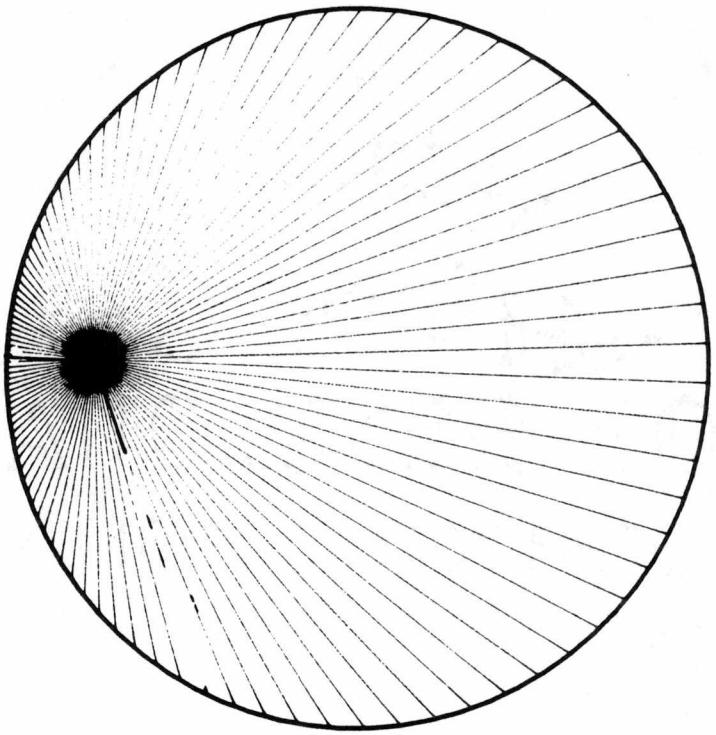


Figure 6.1. A Point Source of Shear Waves Inside an Aluminum Cylinder

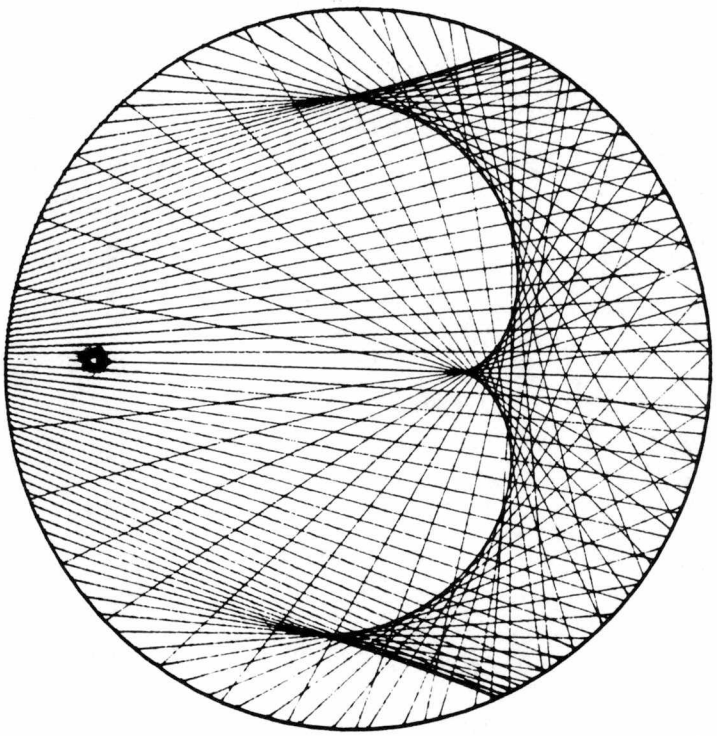


Figure 6.2. Sound Reflected From the Inner Wall

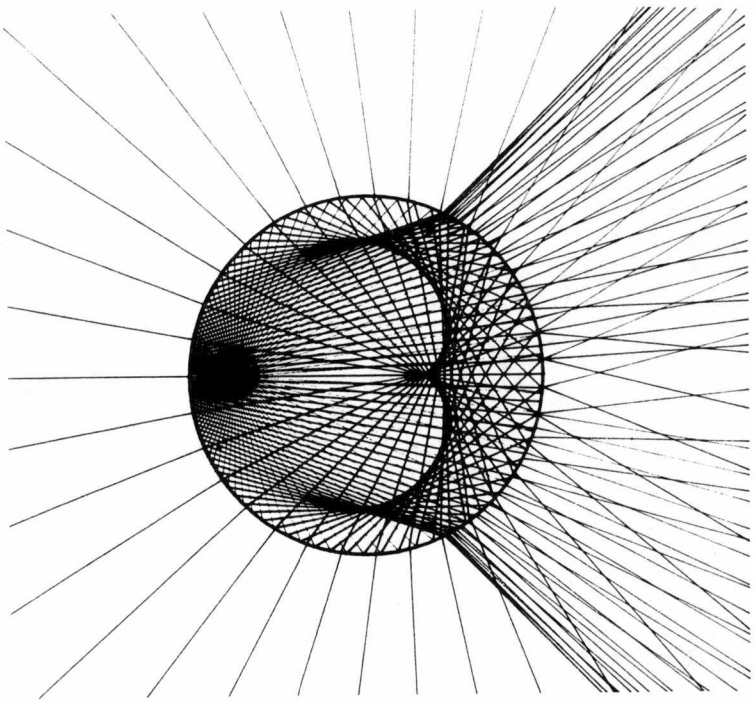


Figure 6.3. Caustic Formed After Refraction into the Surrounding Water

1945]. This states that the intensity produced at A by a point source of waves at B is equal to the intensity that would be produced at B if the same source were to be moved to A. This holds true in the ray approximation, as illustrated by figure 6.4. A point source at A produces a caustic that passes through B and a source at B produces a caustic at A. That is, if A produces an infinite intensity at B then B produces an infinite intensity at A.

A consequence of the fact that these caustics become very straight soon after they leave the sample is that the observed caustic has little dependence on the characteristics of the receiving transducer. Consider a transducer moving across a caustic as shown in figure 6.5. If the transducer can be considered a point source of sound (and therefore, by the reciprocity principle, a multi-directional receiver) it will receive a large signal as it crosses the caustic at A. But, if the transducer produces plane waves it is equivalent to a point source at infinity, apertured by the probe face. In this case the caustic will be received at B where this source at infinity crosses the caustic (and only if the probe is pointing along the tangent to the caustic at infinity). It was mentioned in chapter 4 that for an aluminum rod immersed in water, points A and B are separated by only 0.1 degrees. There is a negligible difference in the behavior between the two extreme kinds of probe.

The fact that caustics are produced by the sound scattered from a defect suggests an ultrasonic defect location technique.

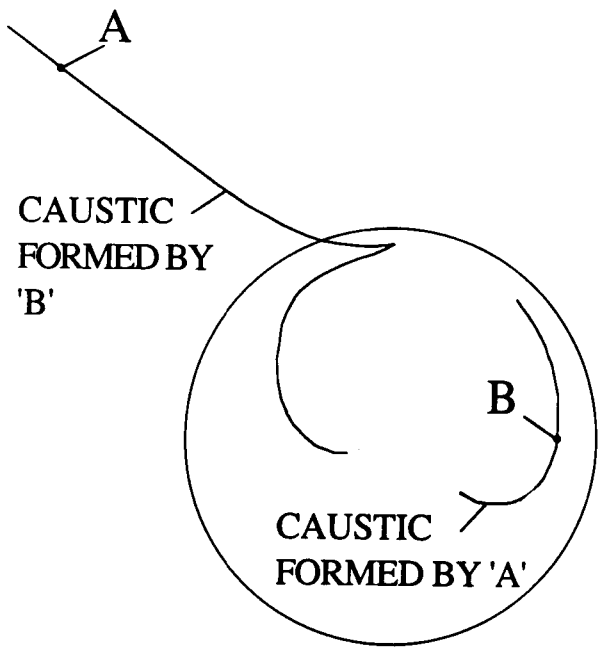


Figure 6.4. The Principle of Reciprocity as it Applies to These Caustics

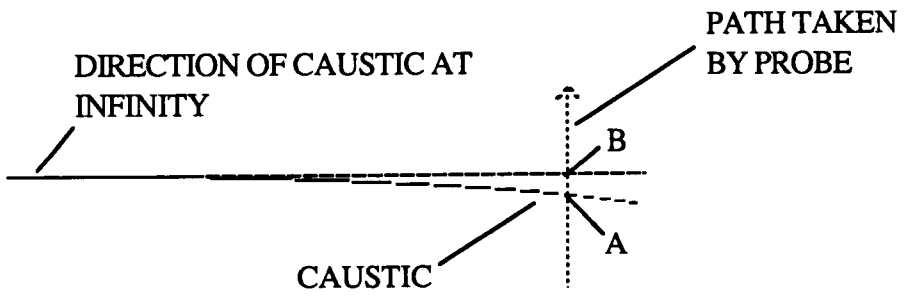


Figure 6.5. A Nearly Straight Caustic

Using two probes configured as in figure 6.6 the region of the sample under inspection is illuminated with ultrasound and the sound field in the surrounding water measured with the receiving transducer. Sound scattered by any small defect in the region illuminated by the transmitting probe will produce a system of caustics as in figure 6.3. If the angular location of the two caustic planes can be identified, the location of the scatterer can be deduced to be on the line of symmetry between the two planes at a radial distance from the axis which can be calculated from the angle between them. This is discussed in detail in chapter 11.

This, as are other N.D.E. techniques arising from this work, is a two-dimensional test. The location of the defects in the axial direction must be found either by some other test or by confining the volume inspected to a thin section of the specimen. This is a common problem in the testing of rods and pipes, alleviated somewhat by the fact that the length of a defect in the axial direction is often less important than its position in the sample.

Experimental

In order to study the sound scattered by a small defect the immersion testing rig was set up in the configuration shown in figure 6.6.

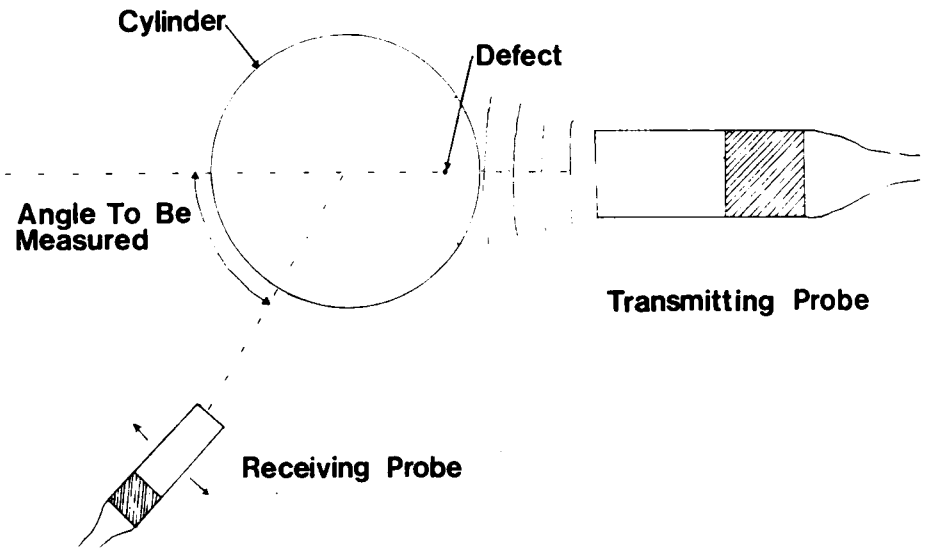


Figure 6.6. Schematic Diagram of Test Setup.

The samples used were commercial grade aluminum cylinders, 78.2 mm diameter and 44 mm high machined to screw onto the rig. To simulate a defect a 1 mm diameter hole was drilled along the length of each sample at differing displacements from the axis.

The 5 MHz transducers were used (the attenuation of sound in aluminum at 20 MHz is too high) implying sonic wavelengths of:

Compression waves in water------- 0.30 mm

Shear waves in aluminum---------- 0.62 mm

Compression waves in aluminum---- 1.27 mm

(Calculated from values of the speed of sound given in the "CRC Handbook of Chemistry and Physics" [WEAST 1986]). This shows that the wavelength is small compared to the dimensions of the sample but large compared to those of the defect, therefore one can justify the use of the ray approximation. The face of the receiving transducer was stopped down to a rectangular aperture 6 mm wide using adhesive backed styrofoam. Using equation 2.2 the near field, in water, is calculated to extend 30 mm from the transducer justifying the assumption that all caustics are formed by rays in the far field.

Using the pulser/receiver in pulse-echo mode each transducer was set normal to the sample face by adjusting both its horizontal and vertical rotational degrees of freedom until the echo from the sample face was maximized. The sample was rotated to the orientation where the defect receives the highest intensity of sound, which was done by maximizing the compression wave echo from

the hole. The receiving probe was offset from normal in the horizontal plane by the angle calculated to point it along the line of the expected caustic.

The pulser/receiver was switched to pitch-catch mode and the various signals received observed on the oscilloscope screen. A sample with a hole 75% of its radius from the center was used for this initial experiment. In order to identify the signal from the caustic the time of flight and amplitude of these peaks were recorded as functions of the angular position of the receiver at 5 degree intervals. Once the caustic was located the profile of intensity across it was recorded by measuring the amplitude of the received signal at one degree intervals.

In order to study the exact relationship between the caustic orientation and the defect location, the separation of the two caustic planes was measured for rods containing holes with various offsets from center.

Taking care not to move either the sample or the transmitting probe the location of the maximum amplitude due to the caustic was found on both sides of the axis of symmetry. The angular offset of the probe was set to that predicted by rotating it about an axis passing through the center of the probe face. The amplitude maximum was located by using the most sensitive voltage setting on the oscilloscope at which the peak could still be observed and moving the receiver so as to maximize the peak height. The receiver location was then read to the nearest quarter of a degree

using the protractor scale. The difference between the two angles thus recorded was taken and divided by two to give a value for the angle indicated in figure 6.6.

For the samples for which they were observable, the above was repeated for the caustics formed by compression waves scattered from the defect.

Results

Three significant signals were recorded in the original survey of the sound field. Their times of flight and amplitudes are graphed as a function of receiver location in figures 6.7 and 6.8. By comparing the times of flight of these signals to those predicted by measuring ray path lengths on ray diagrams, the sound paths responsible for each can be identified as being those shown in figure 6.9.

Signal 3 exhibits the expected properties of a caustic; a relatively sharp peak in intensity dividing the illuminated zone where the signal is small but visible from the shadow zone where the signal quickly disappears.

Figure 6.10 shows the amplitude intensity across the caustic in more detail. The dashed curve shows the predicted first peak of the Airy diffraction function. The peak width was calculated from the relevant caustic radius of curvature but scaled in height and shifted so that the two maxima coincide. The two curves have the same general shape, slightly steeper on the illuminated side than on the shadow side but the width of the measured amplitude profile

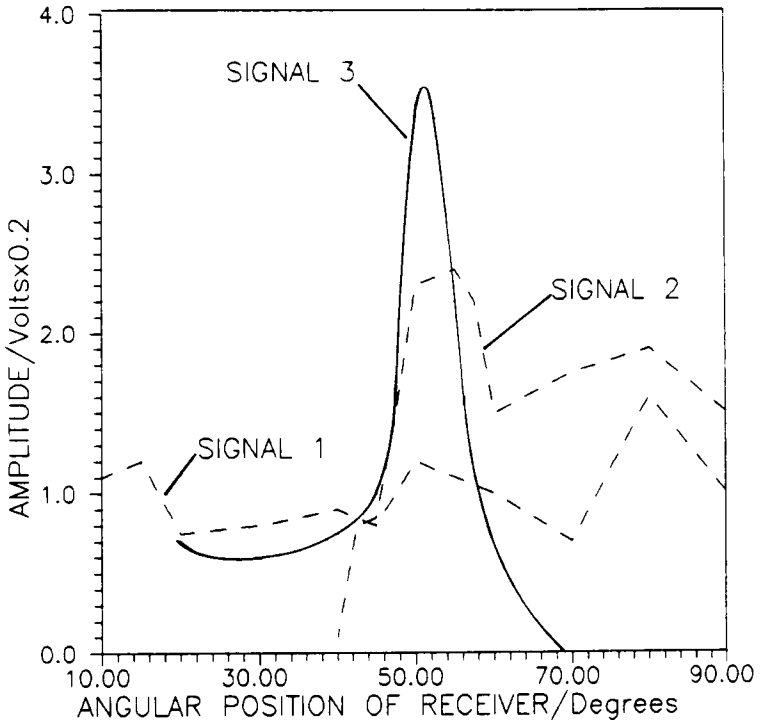


Figure 6.7. The Amplitude of the Received Signals

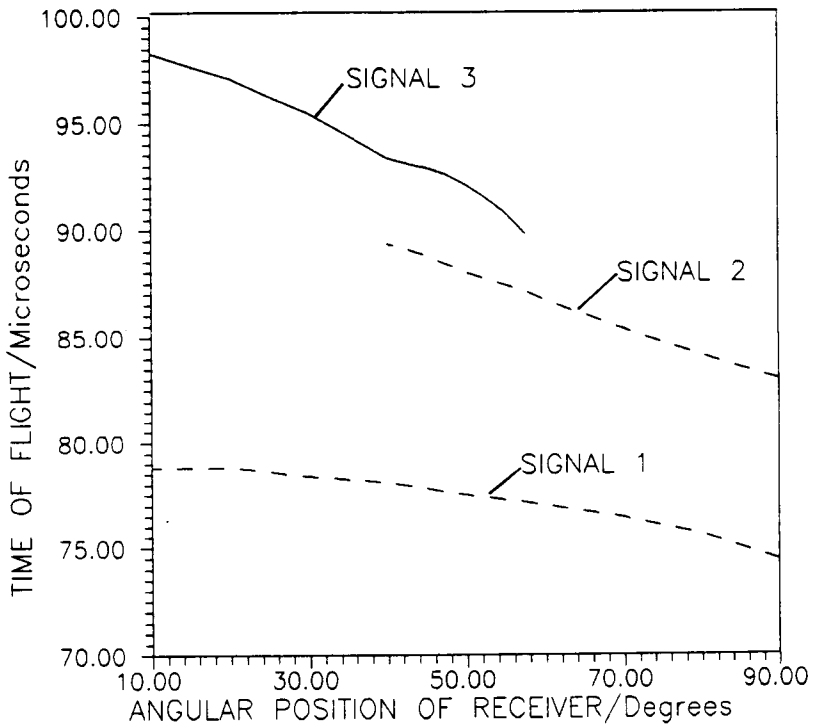


Figure 6.8. The Time of Arrival of the Received Signals

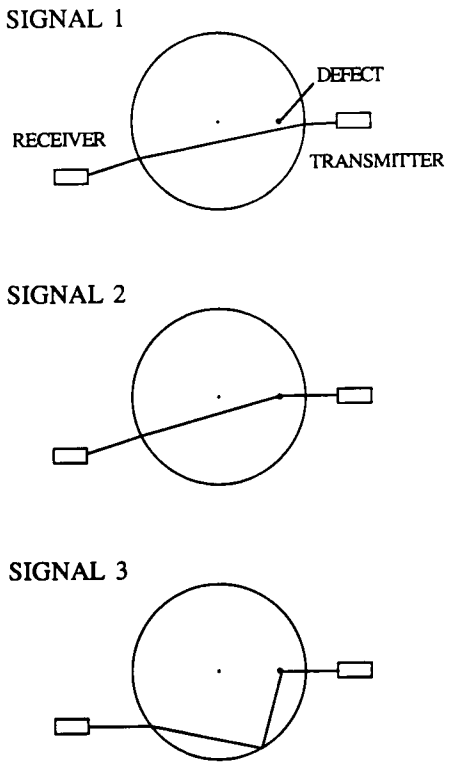


Figure 6.9. The Ray Paths Present

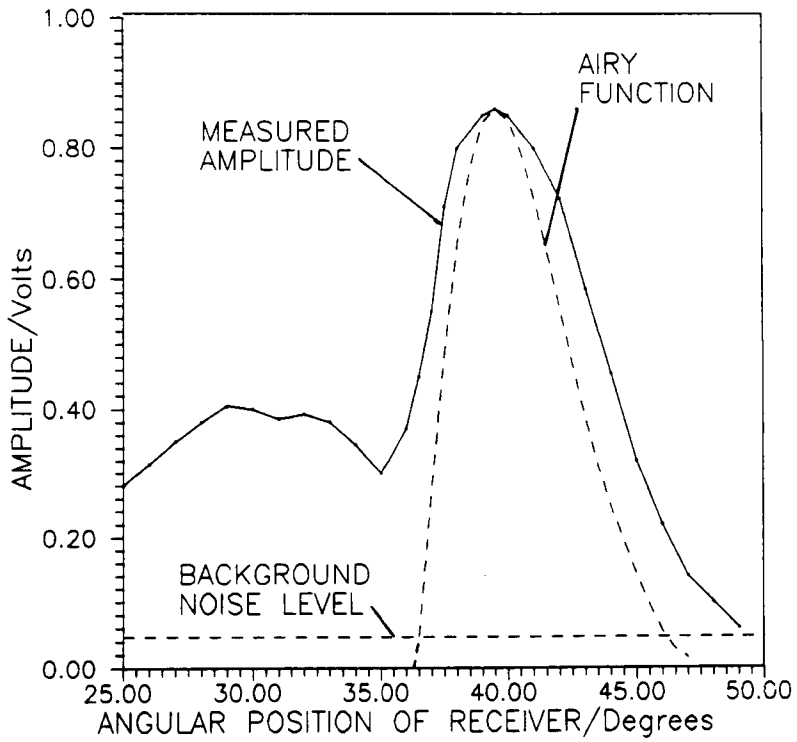


Figure 6.10. The Intensity Profile Across the Caustic

is about 2 degrees greater than that predicted by diffraction theory.

The separation of the caustic peaks as a function of defect location along with the values of this predicted by geometrical acoustics and Airy diffraction are plotted in figure 6.11.

The discrepancies between the measured and expected peak locations are highlighted in figure 6.12 which shows the separation of the amplitude maxima relative to that predicted by Airy diffraction theory. The further the hole is from the center the nearer the peak is to that of the ray approximation, the total change being 4 degrees from one end of the radial position scale to the other. When this same diagram is drawn for the data gathered from the caustics formed by scattered compression waves the curve was sloped in the opposite direction for most of its length (figure 6.13).

Discussion

The caustics formed by scattered sound have been shown to exist and to be observable over a range of defect locations.

The temporal separation of the signals in figure 6.8 is at least three microseconds which, given the one microsecond pulse length, renders the signals readily discernible.

Figure 6.10 shows how as the transducer moves across the caustic into the illuminated zone the signal rises to a maximum over about 8 degrees and then falls to a relatively constant sound

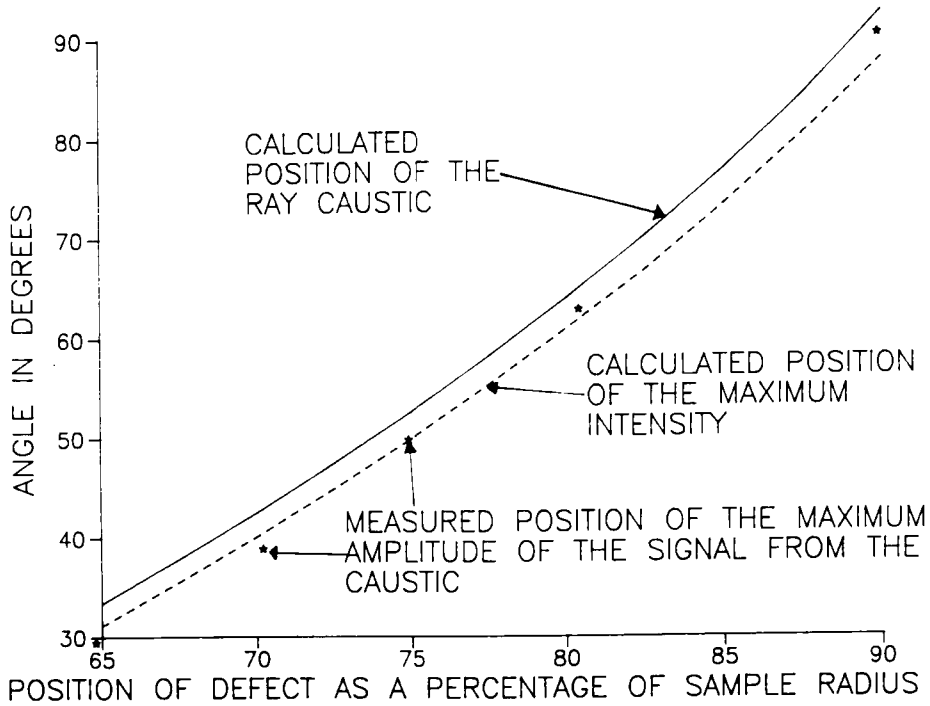


Figure 6.11. The Separation of the Caustics as a Function of Defect Position

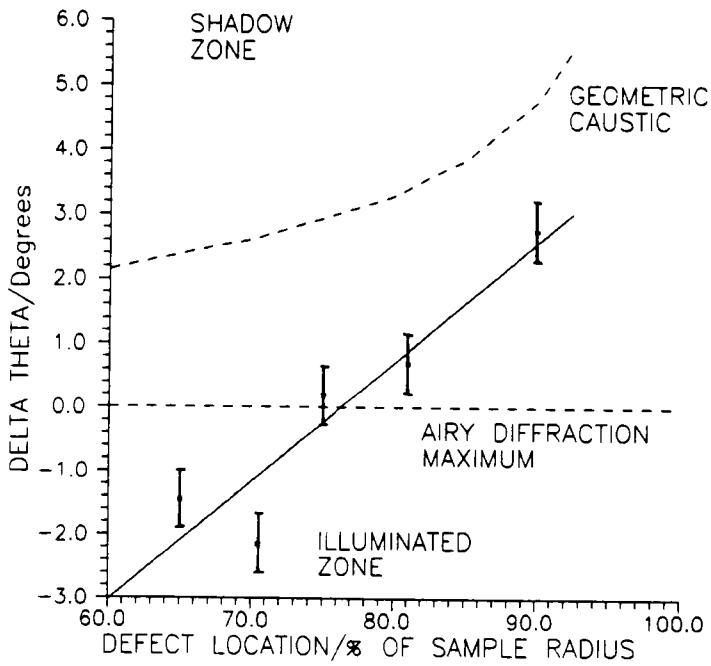


Figure 6.12. Comparison of Results with Airy Theory for Shear

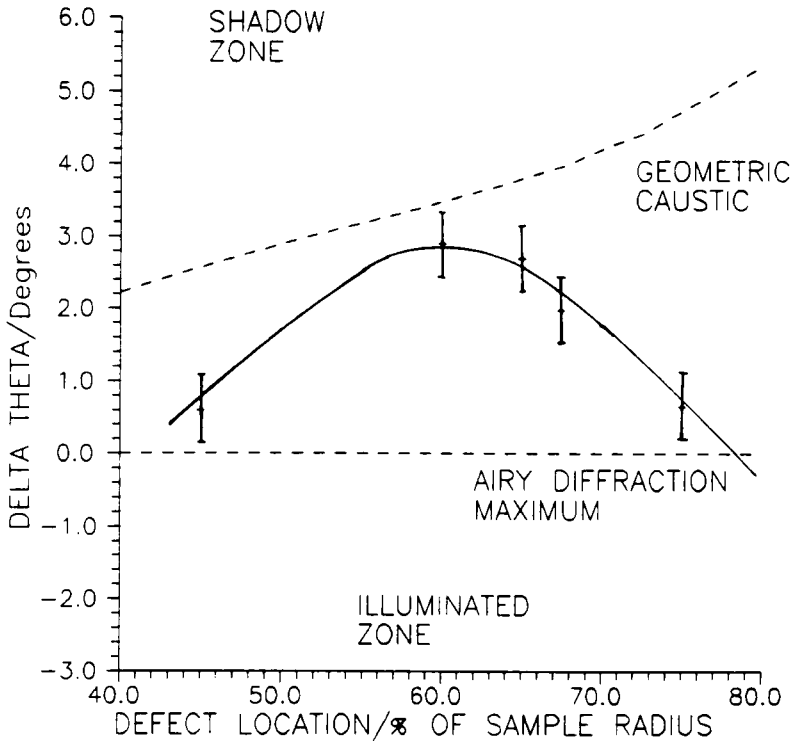


Figure 6.13. Comparison of Results with Airy Theory for Compression

level in the illuminated zone. Qualitatively, the sound profile is much less smooth in the illuminated zone than it is on the peak itself. This is because once past the caustic the signal is composed of contributions from two separate rays which interfere with each other and complicate the measurement of amplitude. The fact that the peak is about 2 degrees wider than the predicted Airy profile can be explained by a combination of two factors. The 1mm diameter of the hole, which leads it to subtend an angle of 2.1 degrees to the sample axis and the width of the receiving transducer, subtending 3.9 degrees (although it doesn't receive with optimum efficiency over all its width).

The correspondence between the caustic separation and defect location is well demonstrated except for the second order effects shown in figures 6.12 and 6.13. These are small enough not to affect the usefulness of caustics in non-destructive testing and could always be incorporated into the calculation of the defect location if such accuracy were required.

The most likely reason for these discrepancies is the fact that the scatterer of sound has a finite size rather than functioning exactly as a point source. Because the diameter of the hole is not much different from the wavelength, the scattering process is very difficult to analyze. For different radial defect positions the direction of the ray which goes on to form the received caustic changes, relative to the incident beam of sound. The most likely explanation for the second order effects is that

the sound field scattered from the hole is strongly dependent on the scattering angle and the mode of sound being observed.

Conclusion

The existence of caustics formed by both modes of sound scattered from a point defect inside a metal rod has been demonstrated. Their width and distance from the line focus of geometric acoustics is close to that predicted by the Airy diffraction theory. Relatively small second order effects were observed in this deviation from the geometric caustic but these are small and smoothly varying enough not to affect any application in N.D.E..

CHAPTER 7

CAUSTICS AND THE SIZING OF EXTENDED DEFECTS

The testing method presented in chapter 6 is, as mentioned, only valid for relatively small defects. Although small voids and inclusions form an important class of defect in many materials, a major task of N.D.E is the assessment of extended defects such as cracks and delaminations. If the defect is large, each point on its reflecting surface acts as a source of sound superimposing many slightly varying caustics on top of one another. The effect of this is to smear out the caustics so that very little information about the defect can be obtained from the loci of the caustics. Also, if the defect is smooth on the scale of the sonic wavelength sharp caustics may be formed by the reflected rays but they will not be related in a simply invertible way to the defect's location and shape.

The existence of caustics can be exploited to locate the ends of an internal crack.

Theory

This technique is best understood by considering the caustic formed by sound incident on a cylinder (as in figure 1.5). As in the preceding chapter two probes are configured as illustrated in figure 6.6. Bearing in mind the fact that the principle of reciprocity means that it is immaterial which probe is the

transmitter and which the receiver, consider the transducer normal to the surface receiving any sound reflected from the defect. If the transmitting probe is moved in an arc around the specimen the caustic will sweep across the crack. As illustrated by figures 7.1 and 7.2 there are two situations of interest; either the crack is entirely inside the shadow zone and therefore not illuminated by any sound reflected off of the sample wall or the caustic is incident on the crack allowing reflections from part of the defect to be observable.

If the point of transition between these two cases can be found then the crack tip is known to be somewhere along the caustic. The location of the end of the defect can then be pinned down by measuring the time of flight of the signal at this critical point.

Identification of the angle at which this occurs is complicated by the facts that the incident beam has a finite width and because, especially if the crack is smooth on the scale of the wavelength, the strength of the received signal is dependent on the angle of incidence of the sound at the crack. If the signal disappears as the probe is tracked around the sample it can be due to either one of three possible factors:

1. The caustic moves so that the crack tip is in the shadow zone

2. The sound is reflected from the crack at an angle which takes it away from the receiver

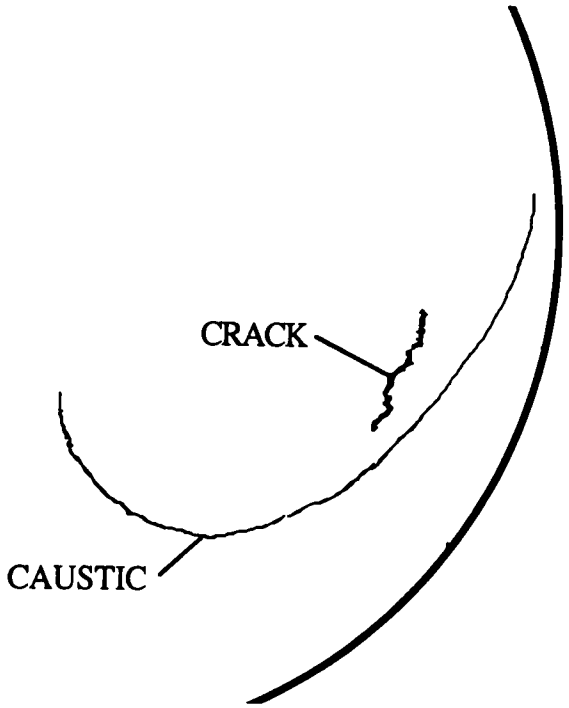


Figure 7.1. Crack Entirely Inside Shadow Zone

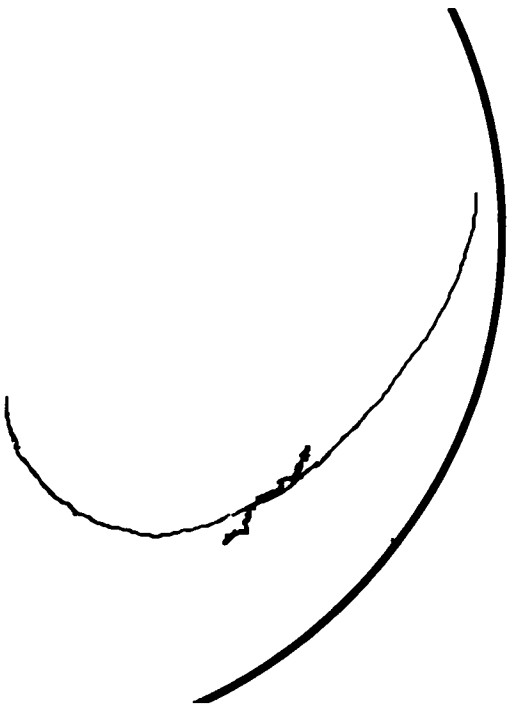


Figure 7.2. Caustic Incident on Crack

3. Due to the finite width of the incident beam, the sound field reflected from the crack is finite and the transducer leaves this region.

In order to locate the crack tips by this technique it is necessary to distinguish between when the signal disappears due to mechanism 1 and not either of the other two.

Experimentally this involves adjusting the configuration of the system to find the minimum angle of separation between the defect and the transducer for which the signal of interest can still be observed. This is because the caustic defines a minimum angle of separation between the transducer and the defect beyond which no sound reflected from the defect can be received.

For consistency with the previous chapter the transducer that can move in a circle around the sample will be referred to as the "receiving transducer" even though distinguishing between the transmitting and receiving transducers is redundant.

Experimental

In order to simulate an internal crack, a longitudinal void approximately 20 mm long and 5 mm wide was drilled into a 76 mm diameter aluminum cylinder. The outward facing edge was smoothed with a file. Because only refections from the outward face are important this is ultrasonically equivalent to a line crack. In order to relate the measured angles to the location of this defect a reference line was scored across the top of the sample passing

through the cylinder axis and the "crack". This reference line was measured to be 172.5±0.3 degrees from the reference point for measuring the angular position of the sample.

The sample was placed on the testing rig and initially the experiment was set up as described in chapter 6.

The pulser/receiver was used in pitch-catch mode and a signal that disappears as the receiving transducer moved closer to the defect found. The transducer was placed at the angle where the signal was about to disappear into the background noise. This small signal was then maximized by adjusting the offsets of both probes from normal (in the horizontal plane). The transducer was again moved to the position where the signal was about to disappear and the maximization process repeated. This was done until the signal could no longer be increased by manipulating the offsets of the probes.

Because this method involves changing the offsets of the probes, their orientation could not be accurately measured. Therefore, the ray paths involved are not known exactly making time of flight measurements unreliable. No measurement was made of the time of flight of these signals.

By this iterative process the minimum angular separation between the transducer and defect is found and the angular position of the probe and the sample where recorded at this point.

This was repeated over a range of angular positions of the sample.

Results

From its time of flight, 3.4 microseconds later than the first sound to arrive, the signal being studied was identified as that which travels to the receiver, entirely in compression mode by the path shown in figure 7.3.

The angular position of the receiver, relative to the sample, at which this signal first appears is plotted as a function of the orientation of the sample in figure 7.4. The x-axis is actually the angular position of the pointer attached on the sample holder. This has a broad, flat maximum corresponding to the signal appearing as the caustic touches the crack tip. Here this occurs at an angle of 82±1 degrees. In order to locate the other crack tip this was done around the other side of the sample and the result of this is shown in figure 7.5. Here the y-axis is the reverse of that for the previous graph because the receiver is being tracked around the sample in the opposite sense. The critical position of the transducer is -63.0±0.5 degrees. One "minimum separation" is actually a maximum in the probe position because the sense of the rotations involved is different in the two measurements.

The fact that neither of these sets of data are smooth stems directly from the irregular nature of the defect. On one side the graph rises to a plateau then falls away but on the other side the signal became too weak to observe during the flat section. This asymmetry is also due to the defect itself not being symmetric.

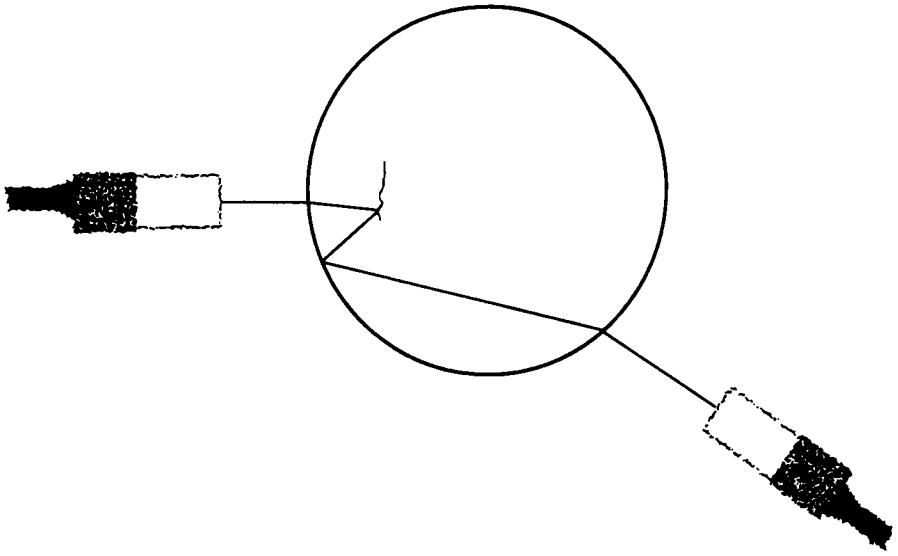


Figure 7.3. The Ray Path of the Received Signal

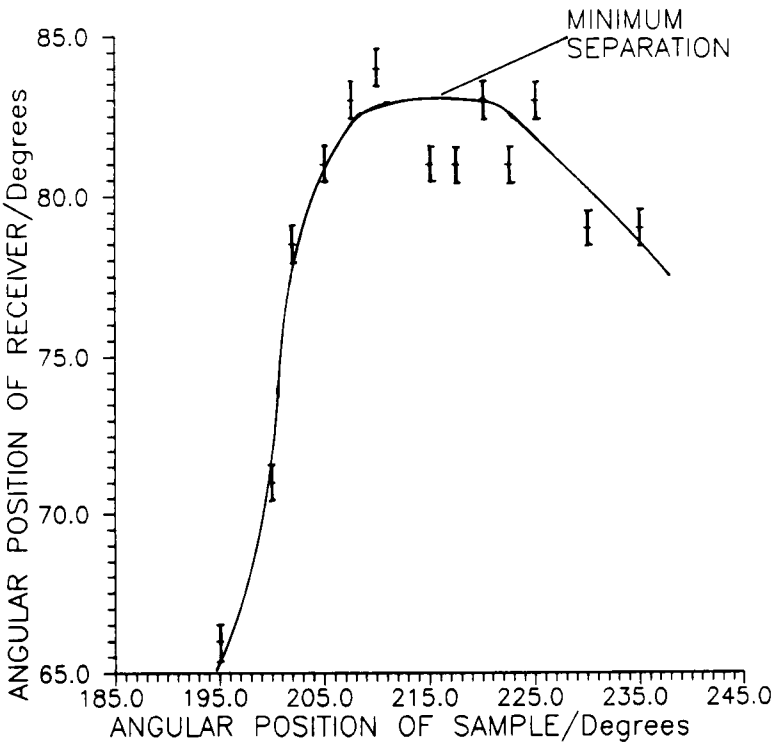


Figure 7.4. Variation of Signal Starting Point with Sample Orientation

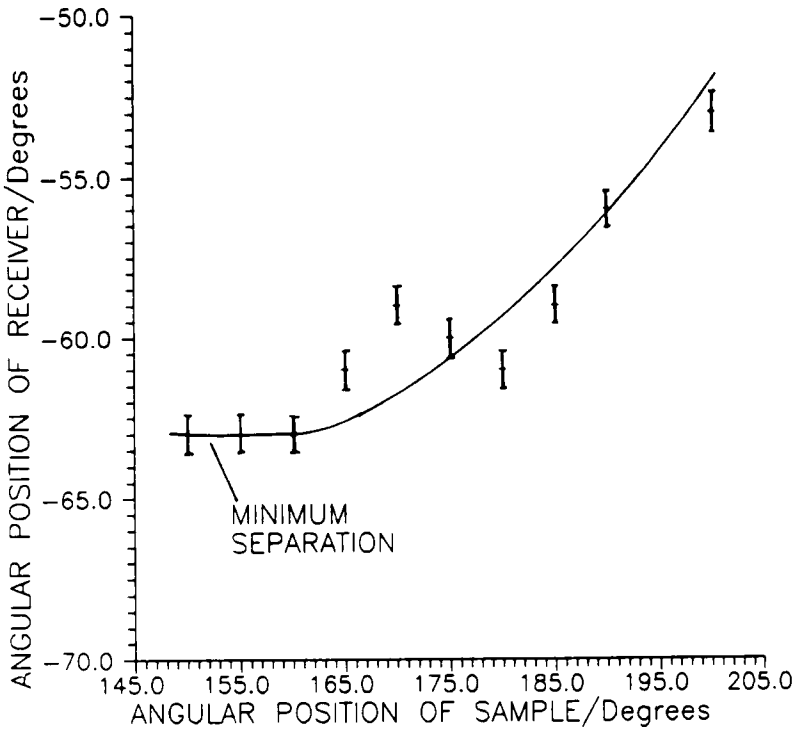


Figure 7.5. Variation of Signal Starting Point with Sample Orientation

These results can be related to the actual position of the crack by constructing the loci of the caustics formed by transducers at these critical positions and superimposing them onto the shape of the defect. Figure 7.6 shows how this was done. The location on the sample of the zero of the angular scale was found to be the position indicated. The two critical locations of the probes, -63 and 82 degrees, are labeled "A" and "B" respectively. The relevant section of the caustics formed by each of these was found by calculating the coordinates of five points along them and joining them with a smooth curve.

Both caustics are very nearly tangential to the defect. The effect of the uncertainty in the identification of the critical probe position is to blur the line caustic into a region containing the end of the defect (figure 7.7). In this case a one degree error is equivalent to a one millimeter uncertainty in the measured defect location.

Discussion

The above results demonstrate that the caustics tangential to the ends of even irregular defects can be found. This allows the location of the ends of the crack to be found either by measuring the echo time of flight of signals from the caustic or by measuring the distance of the crack from the sample edge using a conventional pulse echo technique. (Measuring the time of flight of a normally incident compression wave reflected from the

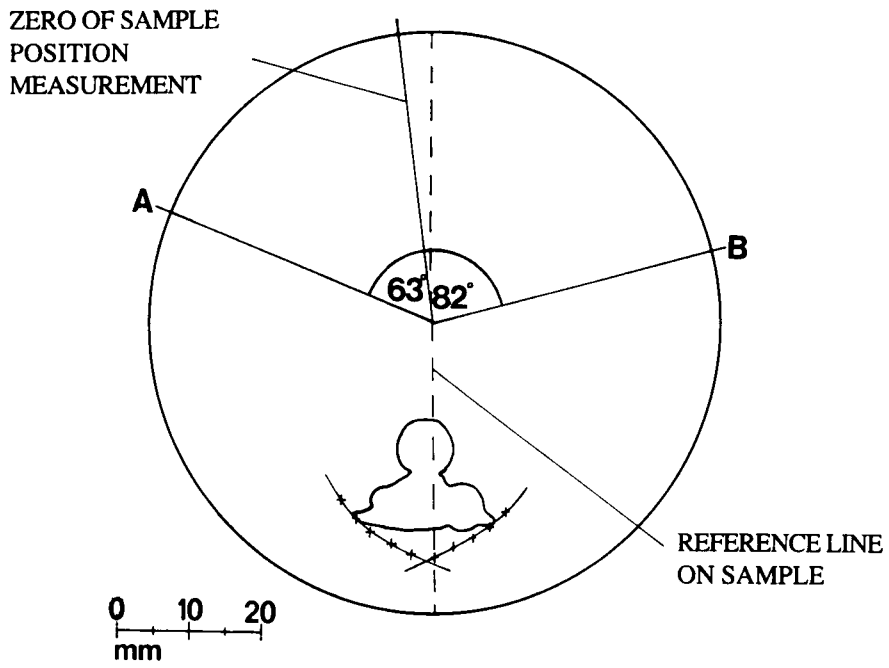


Figure 7.6. Construction of the Caustics Touching the Crack Tip

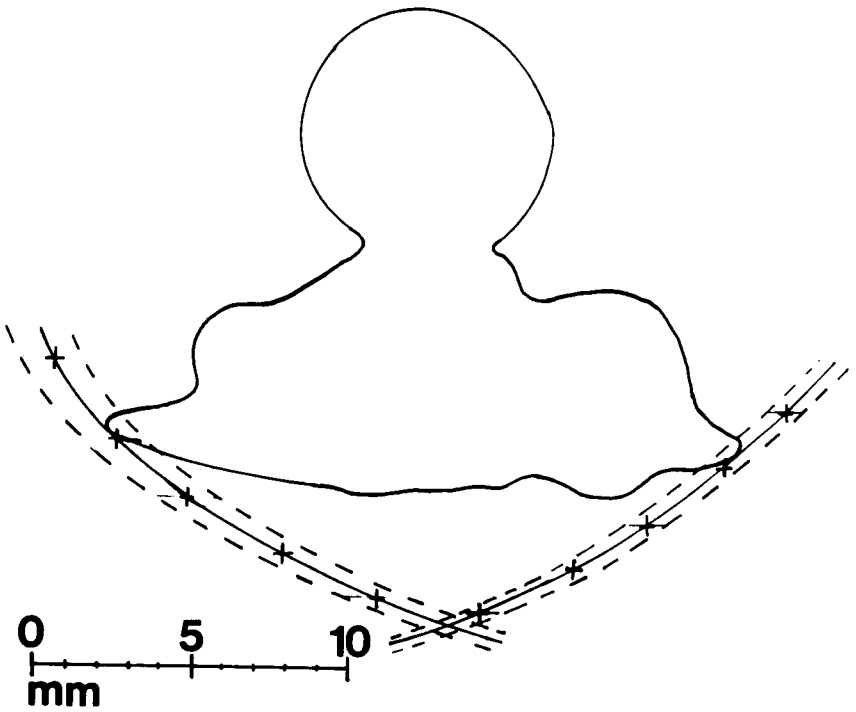


Figure 7.7. The Level of Uncertainty Involved

defect). Also construction of a diagram such as figure 7.7 gives the length of the defect as a function of its radial position. In situations where the threat the defect poses to the integrity of the component increases with its distance from the axis this may be enough information to assess the worth of the sample. Further discussion of the application of this research is given in chapter 11.

Conclusion

A method by which ultrasonic caustics can be used to locate the ends of an internal extended defect has been demonstrated using an irregularly shaped defect.

CHAPTER 8

CAUSTICS AND THE SHADOWS OF SURFACE BREAKING DEFECTS

A very important class of defects in rods and pipes are those which penetrate inward from the outer surface. It is not possible for the caustic to touch the crack tip without at least part of the flaw lying in the illuminated zone. This is illustrated by figure 8.1 where all three cracks are capable of reflecting back sound irrespective of which side of the caustic the crack tip is on. This prevents the application of the technique described in chapter 7 to a surface breaking crack. (The possibility that caustics formed by means other than simple reflection off of the sample walls may satisfy this condition has not been excluded.)

A common means of inspecting surface breaking flaws is to use two probes in pitch-catch mode to search for the ultrasonic shadow of the defect [FILIPCZYNSKI 1966].

Theory

Because of the relatively long wavelength involved the ultrasonic shadow behind an opaque defect is not sharp but "smeared out" by diffraction. As shown in figure 8.2 there is a zone inside the geometric shadow that is illuminated by sound diffracted at the crack tip. But if the crack tip is on the shadow side of a caustic there is no sound present and no diffraction can occur.

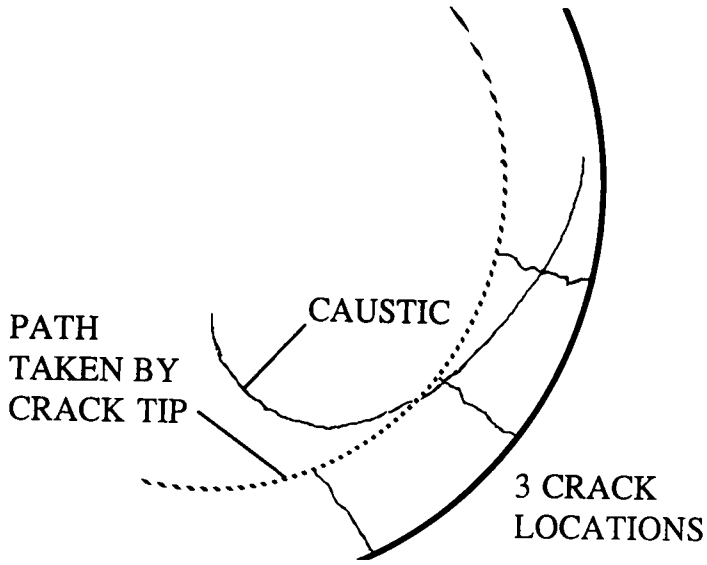


Figure 8.1. Three possible crack locations

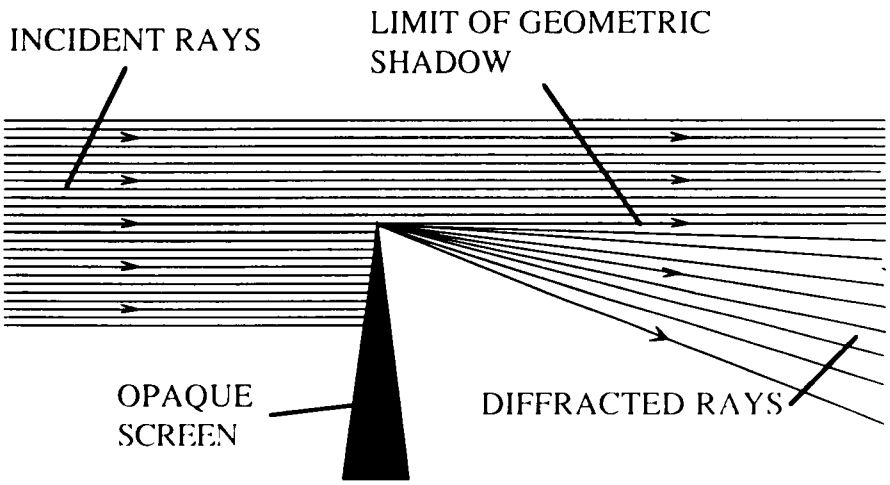


Figure 8.2. Diffraction at an Edge

This concept is best illustrated by describing the testing technique that derives from it.

Figure 8.3 is the same ray diagram as figure 1.5 except that after forming the caustic the shear waves reflected from the inner wall are refracted back out into the water. If two transducers are configured as in figure 8.4, there is one unique ray path between then as indicated. If the test piece contains a surface breaking defect there will be three different cases according to the position of the crack tip (figure 8.5):

Case 1: Crack does not obstruct the path between the transducers.

Case 2: Receiver in the geometric shadow of the crack but the crack tip is on the illuminated side of the caustic.

Case 3: Receiver in the geometric shadow of the caustic and the crack tip is on the shadow side of the caustic.

If the sample of figure 8.5 is rotated clockwise the received amplitude will remain constant in region 1, start to fall as we enter region 2 then, drop off quickly in region 3. By recording the sample position where signal disappears we know when the end of the crack is on the caustic line. From the principle of reciprocity it is immaterial which transducer is the transmitter and which is the receiver, which implies that the same behavior will repeat on the other side of the reflection plane of figure 8.4. This is due to the crack tip moving across the caustic that the receiver would form if it were to transmit. This symmetry

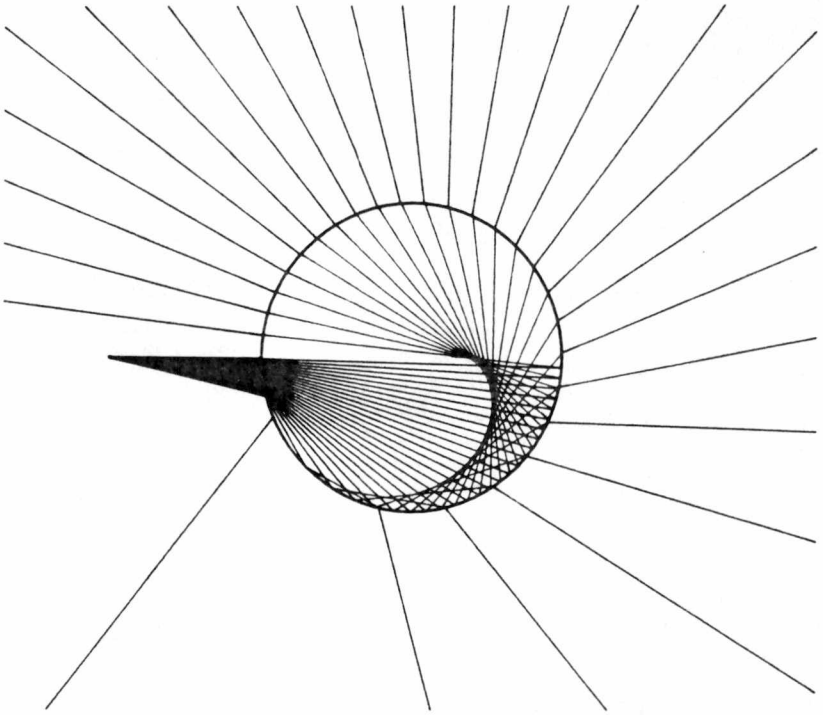


Figure 8.3. Rays Refracted Out After Forming Internal Caustic

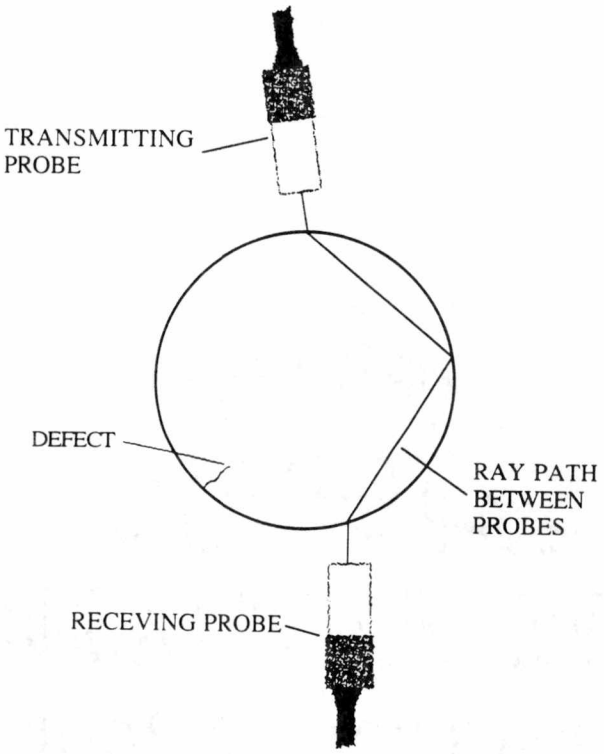


Figure 8.4. Schematic Test Configuration

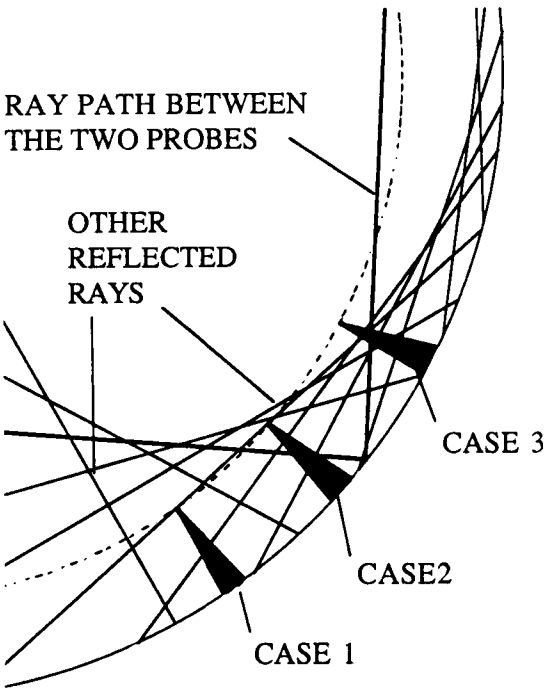


Figure 8.5. The Three Different Situations to be Considered as the Crack Tip Crosses the Caustic

allows the exact location of the crack tip to be found. If the point where the defect breaks the surface is found, either ultrasonically or by some method such as dye prenetrant inspection, the length and orientation of the crack is now known.

Experimental

Surface breaking defects were simulated by machining 1 mm wide rectangular slots into 76 mm diameter aluminum rods. Two samples were made with slot depths of 6.0 mm and 13.5 mm, as measured to the nearest 0.25 mm with a ruler.

The rod was fitted onto the immersion testing rig and with two 5 MHz transducers in the configuration shown in figure 8.4. With the pulser/receiver set to pulse-echo mode the transducers were set normal to the sample by maximizing the echo from its front face. To ensure symmetry between the transmitter and receiver, they need to be the same distance from the sample. This was achieved by moving the receiving probe until the time of flight of the echo from the sample wall was equal for each probe. The pulser/receiver was set to pitch-catch mode and, with the sample rotated such that the slot had no influence, the signal travelling, as a shear wave, via the route shown in figure 8.4 identified. While making sure that the signal continuously varied, the receiver was moved to the angular position desired. The offset of both transducers from normal was adjusted, in the horizontal plane, until the signal of interest was maximized. When this was

done the system should be in the symmetric configuration depicted in figure 8.4; this was confirmed by visual inspection.

All angular measurements were made relative to the transmitting transducer. In order to relate the position of the slot to this scale, the angular position of the sample at which the slot was exactly opposite the transmitter was recorded. This was done by placing a metal straight edge along the line passing through the slot and the sample axis and turning the sample until this line passed through the center of the transducer face. At this point the angular position of the sample was read off via the marker on the sample holder.

In order to normalize subsequent amplitude readings, the maximum signal amplitude that could be found, with the sample positioned such that the slot was out of the way, was read off the oscilloscope screen.

Using the sample with the smaller slot, an overview of the influence of the slot on the signal was gained by measuring the signal amplitude, as a function of sample rotation, over the whole angular range in which the defect has an influence on the signal. This was done at five to ten degree intervals. The position of the slot relative to the transmitter and the signal amplitudes relative to the maximum were then calculated. This was repeated for various positions of the receiver.

In order to study the nature of the shadow of the slot in more detail, without making too many unnecessary amplitude

measurements, the position of the slot was measured at three points chosen to judge where this shadow is encountered. Because they are best understood in the light of the results of the first experiment, the definition of the criteria chosen to define these points is left until the next section.

Picking out particular points on the amplitude profile in this way enabled the nature of the shadow to be studied at several different probe separations. This data was plotted as points on diagrams of the slot position, relative to the transmitting probe, plotted against the separation of the probes. These two variables define the configuration of the system; therefore, information such as when the crack tip touches the caustic and when the receiver is in the geometric shadow of the slot can be described by curves in this two dimensional space.

Results

The variation of the signal amplitude as a function of slot position is graphed for three different angular separations of the probes in figures 8.6 to 8.8. Here the slot position is given relative to the position of the transmitting probe and the amplitude is expressed relative to the maximum recorded with the slot out of the way. The vertical, dashed line at 104.8 degrees corresponds to the calculated points at which the crack tip touches the caustic.

For closer comparison of these intensity profiles they have

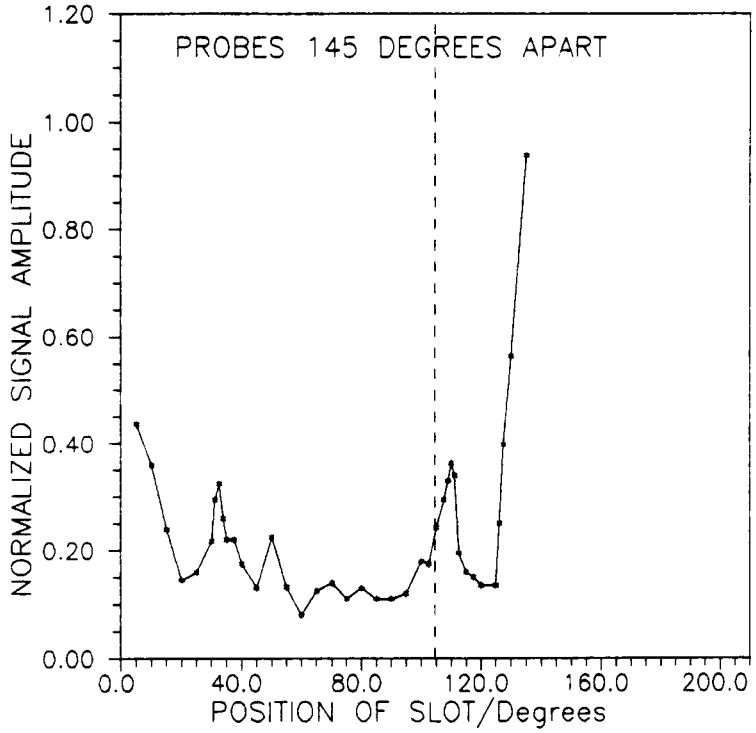


Figure 8.6. Amplitude Profile with Probes 145 Degrees Apart

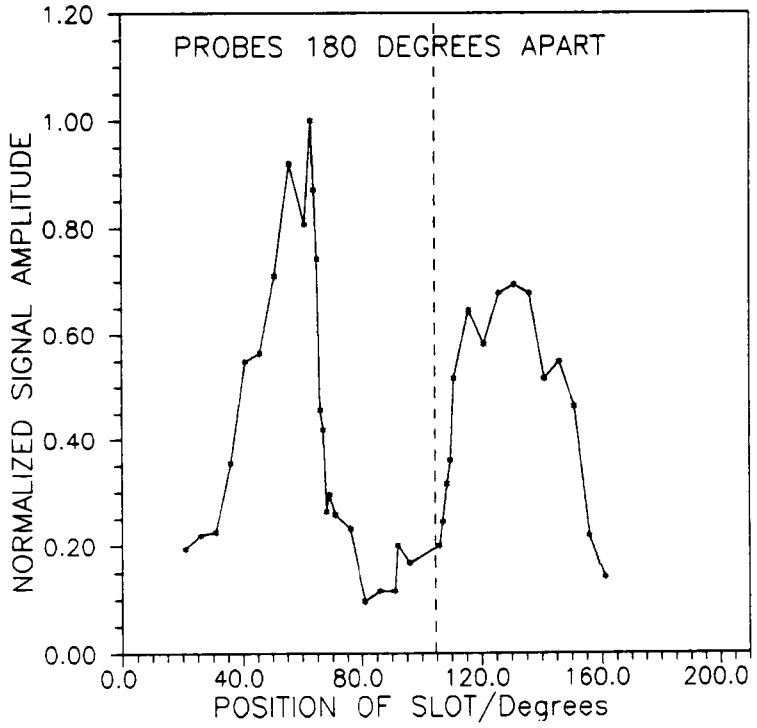


Figure 8.7. Amplitude Profile with Probes 180 Degrees Apart

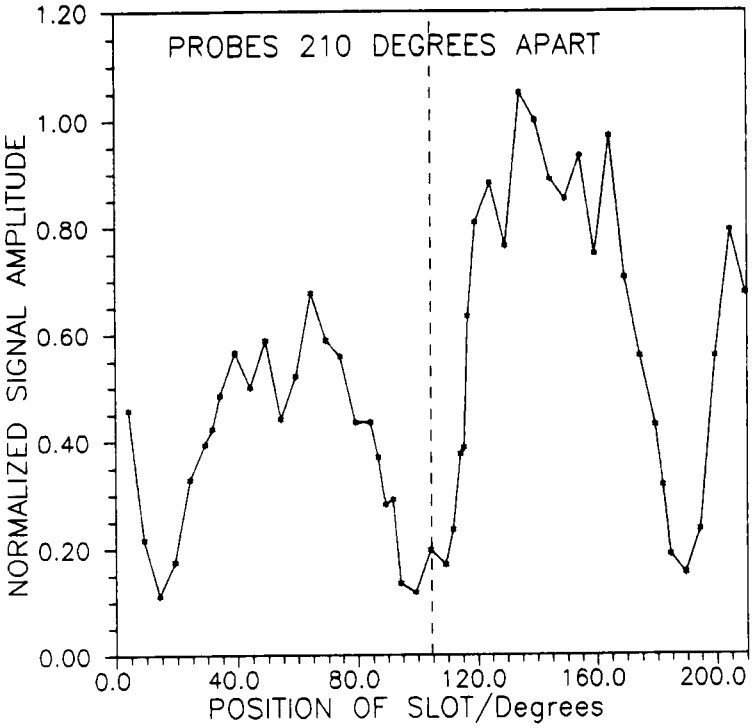


Figure 8.8. Amplitude Profile with Probes 210 Degrees Apart

been plotted on a single graph with the x-axis expanded about 105 degrees (figure 8.9).

All three amplitude profiles start to rise in the vicinity of this caustic angle. The two cases with the wider probe separations have the form of a region of low intensity rising to a plateau of larger amplitude; on the other hand, the other profile has a small peak before the level finally rises. With the probes 210 degrees apart the amplitude starts to rise about 5 degrees further around than it does when the probes are only 145 degrees apart. By inspection of the ray diagram of figure 8.3 it was found that, for this slot, with the probes 145 degrees apart the receiver is always in the shadow of the defect. This implies that the small peak, centered at 110 degrees, seen on figure 8.6 must be produced by a mechanism other than the geometric shadow of the defect.

By the reciprocity principle it should make no difference to the measured intensity profile whether the position of the slot is measured relative to the transmitting or receiving probe. The angular distance of the slot from the receiver was calculated and the intensity profile redrawn relative to the receiver position. Figure 8.10 shows this plot, reversed and scaled for comparison with figure 8.9. These two figures have the same qualitative form but the profiles in figure 8.10 are shifted about three degrees to the right. This is probably due to some source of systematic error in the measurement of the transducer positions that will be eliminated below by averaging these pairs of results.

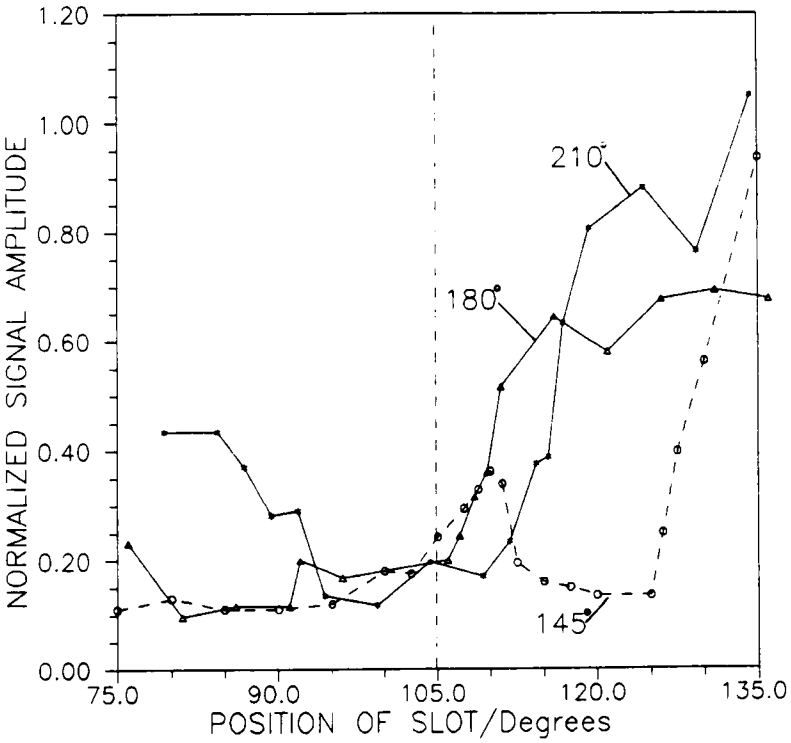


Figure 8.9. The Amplitude Profiles for 3 Receiver Positions.

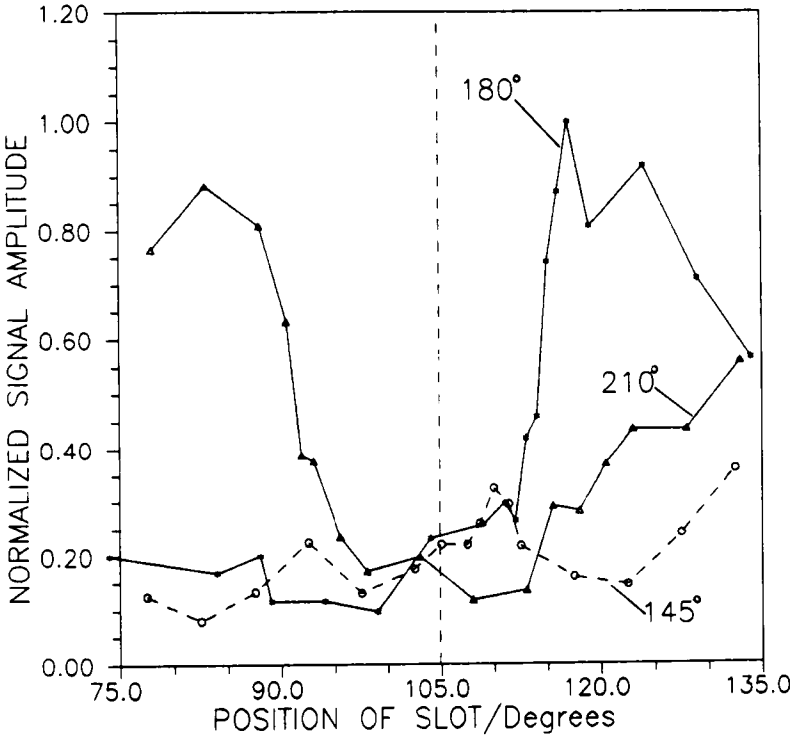


Figure 10. Amplitude Profiles Relative to Receiver

Three criteria were chosen to pick out particular angles on the amplitude profile as the slot leaves the shadow:

1. The angle at which the amplitude is a maximum or reaches its constant high value

2. The angle at which the amplitude is half this maximum value.

3. The angle at which the amplitude is one quarter its value when the slot is out of the way.

For a large range of receiver positions, the slot positions satisfying the above conditions were found. For each criterion the measurement was made twice, once relative to the transmitter and once relative to the receiver, and the mean of the two readings taken. This was done using both samples.

The results of this are graphed for the sample with the smaller slot in figure 8.11 and for the sample with the longer slot in figure 8.12. The crosses correspond to points obeying criterion number one, the circles criterion two and the triangles criterion three. In order to compare the results to the predictions of geometric acoustics, curves corresponding to the boundary of the geometric shadow and the points at which the slot passes through the midpoints of the rays were calculated and plotted on the same graphs. This was done by modifying the ray tracing program. The horizontal line depicts the rotation at which the crack tip crosses the caustic.

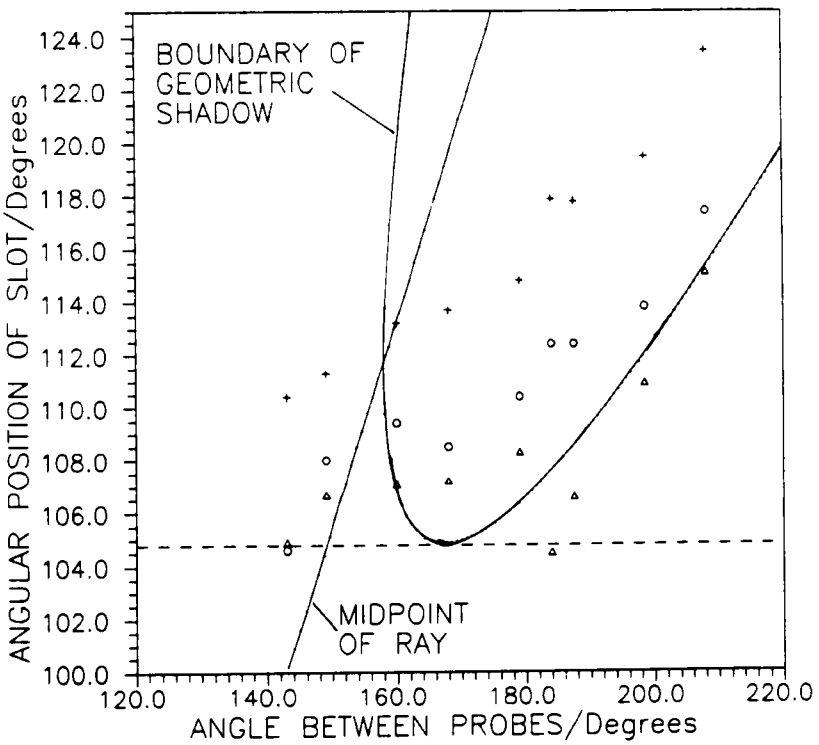


Figure 8.11. System Configuration Diagram --Shorter Slot

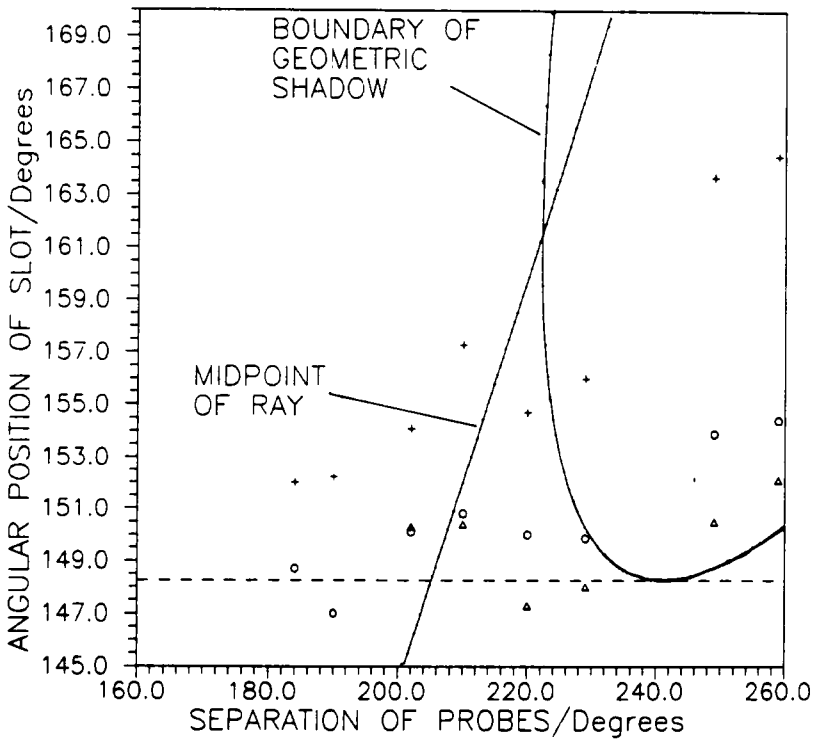


Figure 8.12. System Configuration Diagram --Longer Slot

Discussion

At large separations between the probes the points graphed in figure 8.11L run parallel to the boundary of the geometric shadow. As positions of the triangles and the circles show, as the sample turns the signal starts to rise close to the end of the geometric shadow with the maximum coming about eight degrees later. Data could not be recorded in this region for the long slot because at large separations of the transducers the angle of incidence of the ray path is close to normal which is not favorable for the propagation of shear waves.

Figures 8.11 and 8.12 show that for both samples signals are observed at configurations in which geometric acoustics would forbid the ray path between the probes. For the long slot signals are observed at probe separations up to 40 degrees into the zone of geometric shadow. As the sample is rotated, these signals all start within two degrees of the point where crack tip touches the caustic and reach a maximum about three degrees later. With the small slot signals penetrate about 20 degrees into the shadow these points are not so clearly associated with the caustic.

In the theory section of this chapter it was suggested that diffraction at the crack tip is responsible for these signals and it was mentioned that this effect would turn off as the crack tip crossed onto the shadow side of the caustic. Strong crack tip diffraction would predict that points on figures 8.11 and 8.12 lie on the horizontal line corresponding to where the crack tip

crosses the caustic. For the long slot this is true for the signals in the shadow region. Further evidence that these signals are produced by this diffraction phenomenon is that their intensity profile has the same three degree width predicted by Airy diffraction theory. The results for the small slot don't conclusively show such a dependence on the crack tip crossing the caustic.

Another possible mechanism by which sound can leak into the shadow of a defect involves surface waves. The sound incident on the crack produces a surface wave which travels along the crack and generates a shear wave when it reaches the crack tip. Because of the attenuation of surface waves this effect should be stronger the nearer the incident ray is to the crack tip. For receiver positions that never allow the ray to be free from the slot the lines labelled "midpoint of ray" also show the sample orientations at which the incident ray is closest to the crack tip. Therefore, if the mechanism for the detection of sound in the shadow zone is dependent on how near the incident ray is to the crack tip, the measured signals should show a tendency to follow this path.

This is certainly not true of the signals received from the sample with the long slot. The points in the shadow region on figure 8.11 do not, conclusively, follow either the horizontal line, representing the crack tip crossing the caustic, or the line

on which the ray is closest to the crack tip. This leaves the mechanism by which signals appear in the shadow of the smaller slot unclear.

Conclusion

For the longer crack length signals were recorded in the geometric shadow of the defect which coincided with the crack tip crossing the caustic. This is due to the strength of diffraction around the crack tip increasing as it encountered the region of high intensity near the caustic. For the sample with a shorter slot signals were still recorded inside the shadow of the defect but it was not clear whether or not they were associated with the crack tip crossing the caustic.

CHAPTER 9

ULTRASONIC IMAGING UTILIZING CAUSTICS

Objects without cylindrical symmetry can be tested if instead of using the inner wall of the sample, one uses a cylindrical reflecting dish to focus the sound.

Theory

Rays from a point source outside a circular reflector will go on to form a caustic very similar to that seen in a coffee cup (figure 9.1). This can be used as the basis for an ultrasonic imaging system.

If the transducer shown in figure 9.2 is scanned along an arc concentric with the reflector the caustic will scan across the specimen without changing shape. Because the shape of the caustic and the time of arrival of sound at each point along its length can be calculated, it is possible to construct an image of the object. This is done by recording the amplitude and time of flight, of each echo coming back from the object, as a function of probe position and making the assumption that all echoes come from the caustic. Each recorded time of flight leads to a possible location along the caustic. Knowledge of the location of the caustic allows each echo to be related to a possible reflecting point on the object. Because the image is reconstructed using one spatial coordinate of the transducer and the time of flight of the

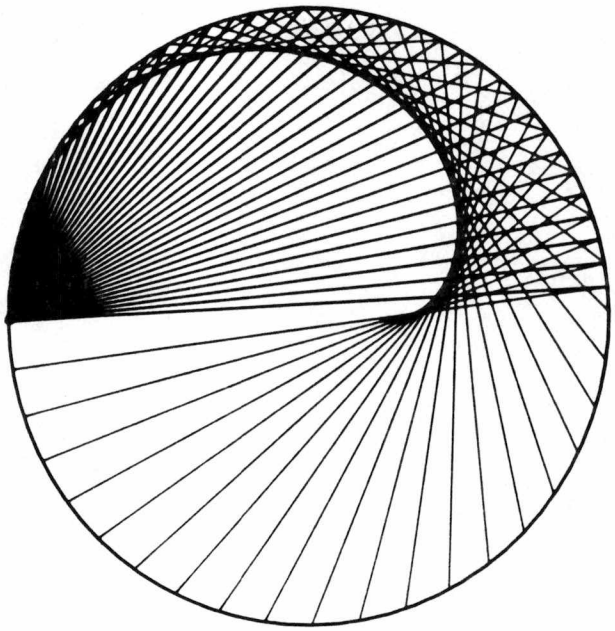


Figure 9.1. Caustic Formed by Rays Reflected from Dish

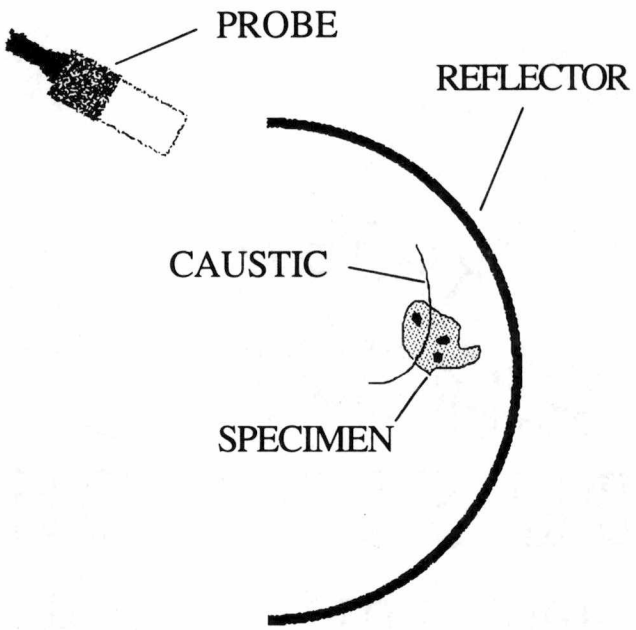


Figure 9.2. Schematic Test Setup

echoes, this technique is akin to an ultrasonic B-scan test.

Using the caustic as a probe in this way is essentially a high depth on field acoustic microscope. Instead of scanning a point focus across an object the focus is a line and the image is numerically reconstructed.

Because of the distortions that will be created by high acoustic refractive index objects (such as metals and ceramics) this kind of test is best suited to medical applications or to the inspection of low density materials such as aerospace honeycomb. Also, high frequency ultrasound scarcely penetrates most materials, but is capable of forming sharply defined caustics that can image a rough material surface with high resolution and depth of field.

The effectiveness of this imaging technique depends on echoes formed due to sound focused at the caustic being dominant over echoes arising from other sources. If the object contains smooth reflecting planes signals from favorably oriented planes lying in the illuminated zone will be as large as those from points on the caustic leading to spurious image points being calculated.

The depth of field of the image is limited by the finite width of the incident beam which implies that only a segment of the possible caustic is actually illuminated by sound. As one moves away from the illuminated part of the caustic the dominant factor in the intensity of the wavefield ceases to be the focusing effect of the caustic and becomes the profile of the incident

beam. This causes the image to be distorted and resolution to be lost. This depth of field is in the radial direction; in the circumferential direction the field of view is limited only by the dimensions of the reflecting dish.

The purpose of the experimental work is to demonstrate the feasibility of this image formation technique, assessing the effect of echoes not originating from the caustic and the finite beam size.

Experimental

The reflecting dishes were two 10 mm thick steel pipes of semicircular cross-section and inner diameters of 205 mm and 130 mm. These could be fitted to holes drilled in the base of the rig such that they were concentric with the axis of the probes' movement. The large dish was used in conjunction with a 5 MHz transducer and the smaller dish with a 20 MHz transducer. Throughout these experiments the pulser/receiver was set to operate the transducers in pulse-echo mode.

In order to demonstrate the ability to image the internal structure of objects, the apparatus were set up with the large dish and the 5 MHz transducer. The transducer was placed at a radial position equal to the radius of the dish.

In order to maximize beam divergence and therefore the depth of field the face of the 5 MHz transducer was stopped down to a 1 mm wide vertical slot using adhesive backed styrofoam. Given the

0.3 mm wavelength of 5MHz sound in water, equation 2.2 predicts a far field beam divergence of 20 degrees. Making the probe face any smaller reduced the intensity of the received signals to unacceptably low levels.

The depth of field was estimated by measuring the angle and time of flight at which the maximum echo from a vertical 3mm diameter aluminum rod, placed in the vicinity of the caustic, occurs. This was done over the largest possible range of angles of offset from the normal that the probe holder would allow to be accurately measured. The dependence of these two quantities on the offset of the probe gives a measure of the angular range over which rays are emitted from the transducer allowing the illuminated length of the caustic to be found.

The object to be imaged was placed on the sample holder in the correct position to reflect sound from the caustic. The amplitudes of the echo signals were recorded as a function of their time of flight and the angular position of the probe. This was simplified by dividing the temporal range into one microsecond intervals and recording the maximum signal amplitude within each of these. The signal was observed at intervals of at least one degree over the whole arc for which echoes from the sample could be observed. The data was written into a computer file so that it could be processed by the image reconstruction software.

As a relatively easy test of image formation ability, a 30 mm square metal block, covered on two sides with glass paper was

imaged.

To demonstrate the imaging of the inside of an object a sample of aerospace honeycomb consisting of aluminum hexagons of side 4 mm was tested and the computer generated images compared to the actual object.

In order to demonstrate the imaging of surfaces at higher frequencies the 20 MHz transducer was used in conjunction with the 130 mm reflecting dish.

In order to produce the same beam divergence as was observed for the 5 MHz sound the transducer would have needed to of been stopped down to a width of 0.25 mm. Because of the high attenuation of sound at this frequency, even with the full transducer face, the received echoes were faint, making it impractical to stop the probe down further. Instead, the depth of field was increased by moving the probe out to the largest radial distance from the axis that the design of the rig would allow (150 mm). The radial depth of field was estimated, as before, by measurement of the dependence of the position and time of the amplitude maximum on the offset of the probe.

In order to gain more precision than is possible by measuring angle off of a protractor scale a micro-translation stage was used to move the sample across the caustic. This was fixed to an optical rail placed on top of the testing tank and the sample suspended in the water by a system of rods. This allowed translation of the sample to a precision of 10 μm.

Because it is corrugated, irregular in one dimension yet smooth in the other direction, a wooden surface was chosen to test the ability to image the section of a rough surface. A piece of maple was broken and the fracture surface scanned across the caustic. The amplitude profile was measured at 0.25 mm intervals, the signal being divided into time intervals 0.1 μs long.

As a more difficult test the fracture surface of a 13 mm wide steel bar broken by impact at low temperature was imaged.

Results

In the preliminary experiment to estimate the depth of field the location of the maximum echo from the vertical rod was unchanged as the offset of the probe from normal was swept over the full 30 degree range permitted by the transducer holder. This is consistent with the 20 degree far field beam divergence predicted for this probe. The rod was 75% of the radius of the dish from the center. For a source at this radial position a 30 degree change in the offset from normal of the received caustic is equivalent to a change in the radial position of the source of 15%. The radial depth of field is thus 15% of the reflectors radius, which for the larger reflector is 15 mm.

The first object to be scanned by the caustic was the corner of a metal test block. The data was processed by the image reconstruction software and figure 9.3 is a photograph of the V.D.U. output. The straight edges of the block and the right

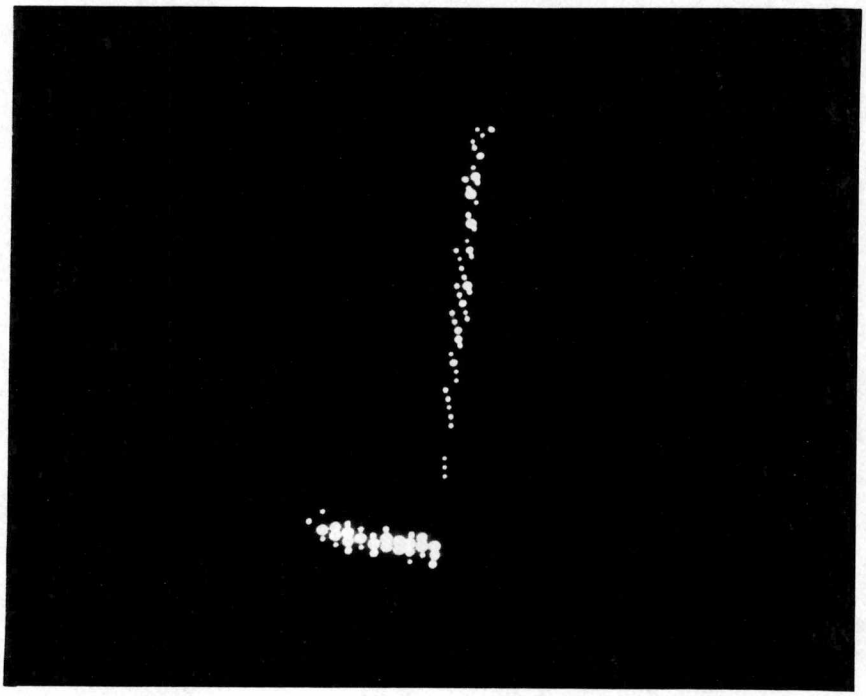


Figure 9.3. A Computer Generated Image of a Right Angled Corner

angled corner are clearly visible.

The computer program was written so that the brightness of the dot drawn on the screen is proportional to the intensity of the received signal. Due to the photographic developing process these dot are larger than those due to weaker echoes. This means that it is clear from a photograph of the screen which part of the sample gave the strongest reflections. Figure 9.3 shows that one edge gave much stronger echoes than the other, this is because that face was inclined closer to normal to the direction of the incident caustic.

For the sample of aluminum honeycomb data was taken at 339 different points. The image constructed from this is shown in figure 9.4 along with an equivalent photograph of the actual sample on approximately the same scale (figure 9.5). Although only planes in one of the three orientations produced strong echoes the hexagonal form of the sample can be seen. There are some faint echoes from other planes. The radial depth of field estimated from this image is about three hexagonal cells or 20 mm, 30% greater than estimated from the initial experiment but still consistent with a 20 degree beam divergence. In the circumferential direction the depth of the image is limited by the attenuation of the sound by the sample, this can be overcome only by using a more powerful source of sound.

For smaller dish and 20 MHz sound the result of the preliminary experiment was that the position of the maximum of the

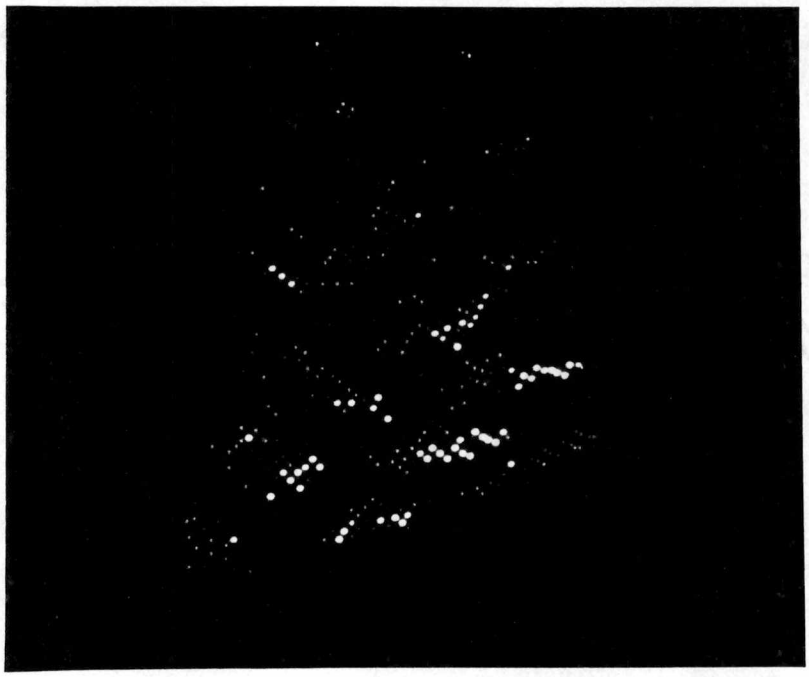


Figure 9.4. Computer Generated Image of an Aluminum Honeycomb

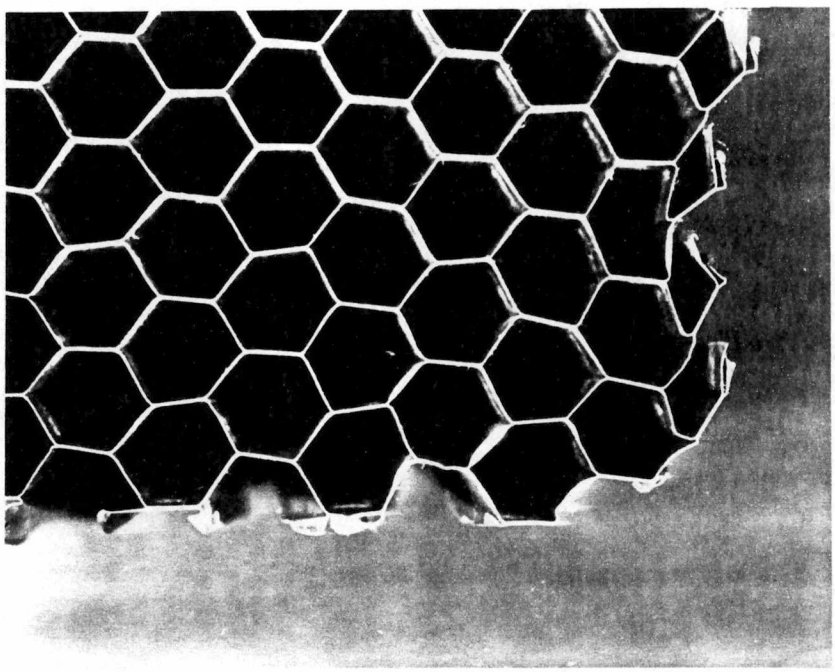


Figure 9.5. An Aluminum Honeycomb

echo from the calibration rod was unchanged over a range of offsets of 3.5 degrees. This was calculated to be equivalent to a radial depth of field of about 4 mm. Although relatively small the caustic is still long enough to allow the imaging of most rough surfaces.

Two fracture surfaces, one wooden and one metallic, were imaged. Figure 9.6 shows the imaged formed by scanning the caustic across the first 15 mm of the sample photographed on the same scale in figure 9.7. The images compare quite well; some 1 mm wide protrusions corresponding to the grains of the wood can be seen in both images in matching positions.

A 9.5 mm length of the 13 mm wide steel fracture surface was scanned. The ultrasonic image can be compared to the actual specimen by means of figures 9.8 and 9.9. Little detail can be mapped from one image to the other beyond the fact that both rise in the middle. There is a line of bright points seen emanating from the right end of the image of figure 9.8 with no equivalent feature seen on the sample. This is due to echoes from the corner of the sample, an efficient reflector of sound, being received when it is away from the caustic but inside the illuminated zone.

Discussion

The results demonstrate that the assumption that the sound field is zero everywhere except on the caustic has enough validity to be used for the construction of images.

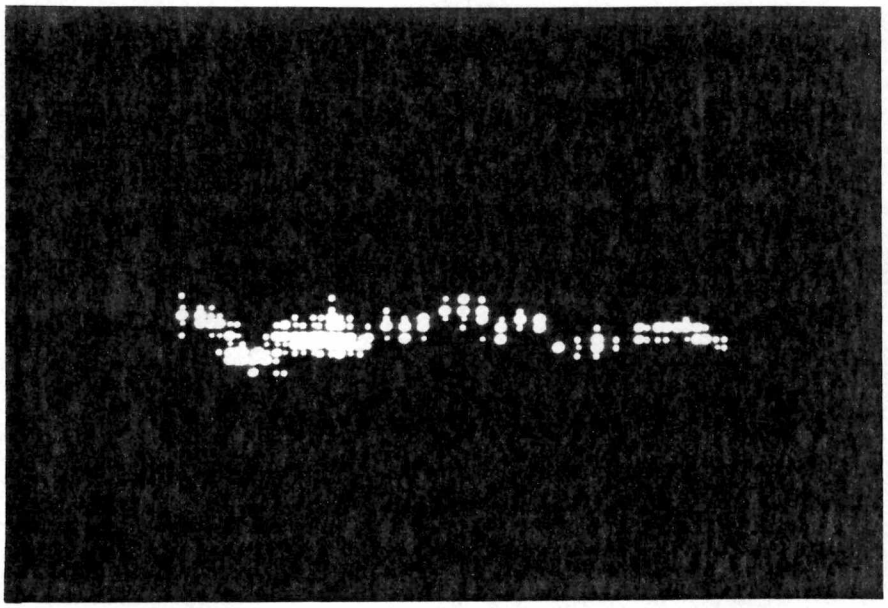


Figure 9.6. Computer Generated Image of a Wooden Surface

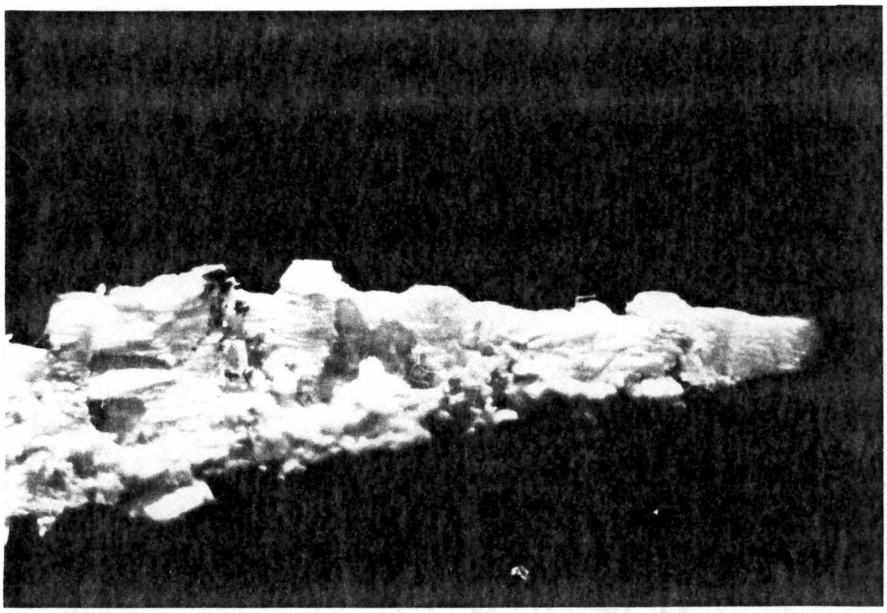


Figure 9.7. A Wooden Fracture Surface

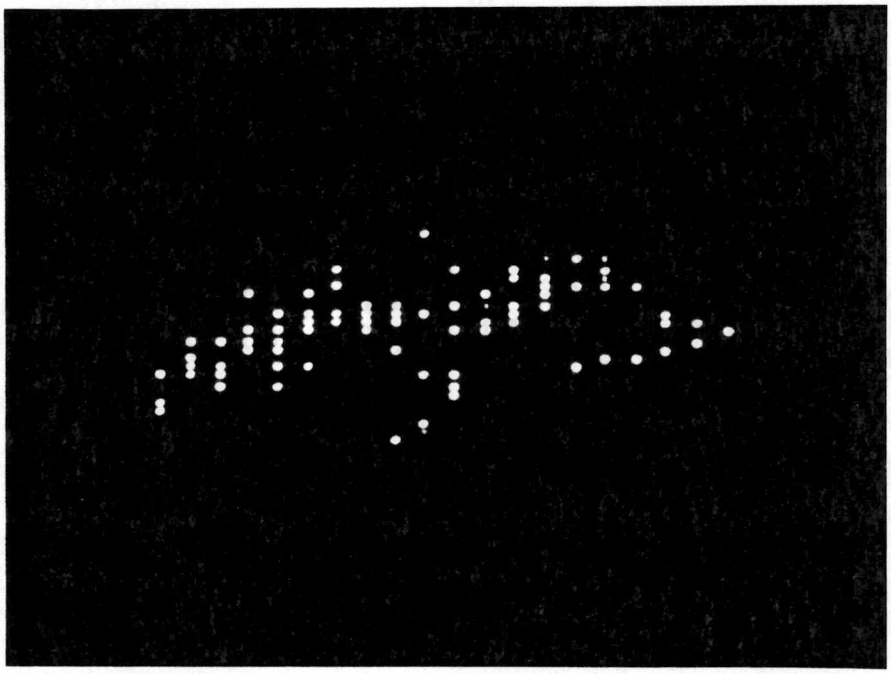


Figure 9.8. Computer Drawn Image of a Metallic Fracture Surface

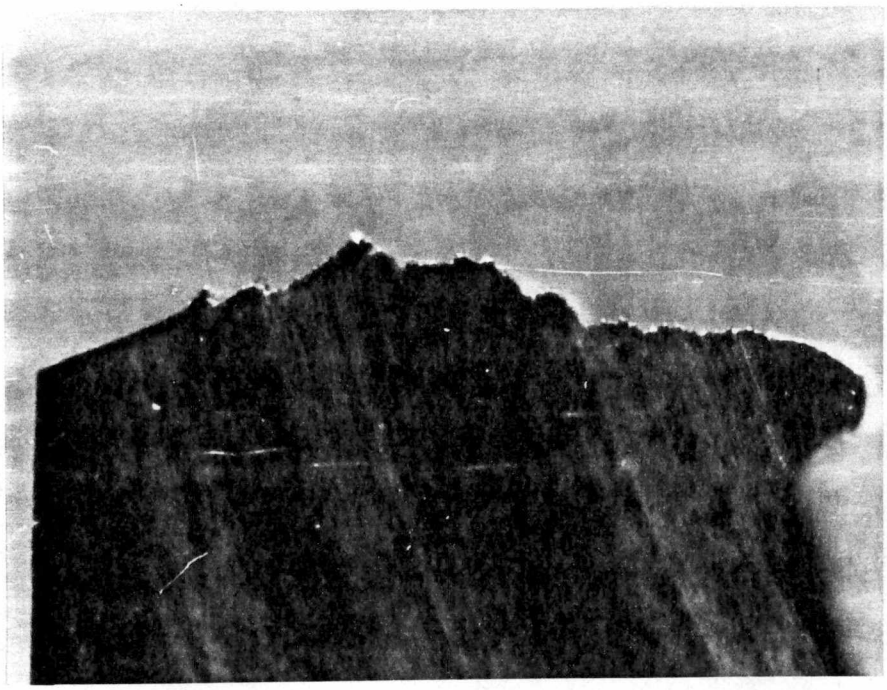


Figure 9.9. A Metallic Fracture Surface

The image of the aluminum honeycomb is spoiled by the fact that only planes facing in one of the three directions are clearly visible. This illustrates a common problem in ultrasonic testing when the specimen or defect being looked at is smooth. In these situations the intensity of the echo is often highly dependent on orientation making it difficult to gather reliable information about the reflecting object.

It is in these situations that one would expect the most confusion of the image due to parts of the object, away from the caustic, but favorably oriented to reflect back echoes. Figure 9.4 shows no evidence of this happening.

At the higher frequency, figure 9.6 demonstrates that this technique is capable of imaging surface features at least down to the millimeter scale. The attempt to image a metal fracture surface was not so successful; the image was difficult to relate to the object responsible and contained several spurious lines due to reflections from inside the illuminated zone.

The main problem with this technique is that it is essentially two dimensional and the image is the superposition of images formed from echoes from different heights on the specimen. This is not so much of a handicap if the sample is relatively smooth in the direction parallel to the axis but it can totally confuse images of specimens with genuine, 2-dimensional, roughness. This could be overcome by having a slit aperture in front of the sample so that only a thin section of it is imaged.

The radial depth of field was limited in both cases by the characteristics of the beams produced by the transducers used. In general, the formation of caustics requires a smoothly varying illumination (that is, the opposite of diffuse illumination). This is best achieved ultrasonically using either a small point source or a wide parallel beam of sound. The field of the images could be increased by using either a transducer with a convex face or placing a convex lens in front of the probe to produce the desired diverging beam of sound.

Conclusion

It has been shown that an image can be formed by scanning a caustic through an object and numerically processing the received signals. In order to optimize this method more suitable transducers are required.

CHAPTER 10

A HIGH DEPTH OF FIELD OPTICAL MICROSCOPE

As was mentioned in chapter 9 the use of a caustic rather than a point focus can greatly increase the depth of field of an instrument. A method has been invented by which this principle may be applied to optical microscopy. Although only preliminary experiments have been done the theory behind this is presented here.

Theory

Consider the optical system shown in figure 10.1. A cylindrical mirror forms a caustic which draws a straight line of high intensity where it meets the specimen. By the principle of reciprocity, if the light source is replaced by a light detector it will detect light originating from the same line on the sample particularly efficiently. If two such optical systems, one transmitting and one receiving light, are placed at right angles it is possible to image a single point on a specimen (figure 10.2). This is because the line on the sample illuminated by one mirror is perpendicular to the line that can be "seen" by the other half of the optical system (figure 10.3). The light intensity at the photometer is proportional to the reflectivity at the point of intersection of these two lines. An image of the sample can be formed by scanning it across the plane of its

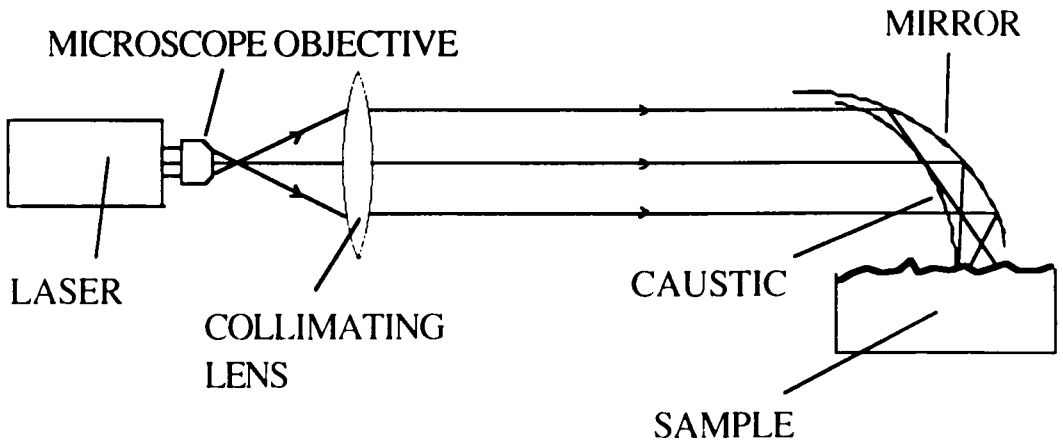


Figure 10.1. The Optical Caustic Formed by a Cylindrical Mirror

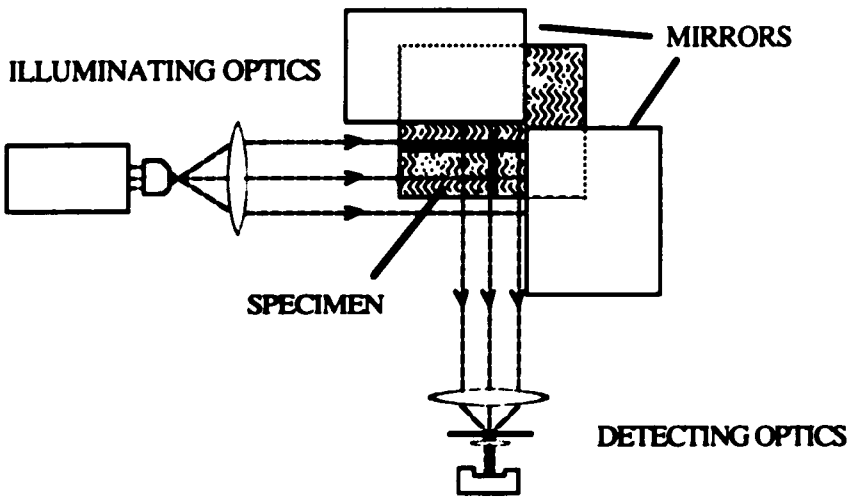


Figure 10.2. Schematic Diagram of the Microscope

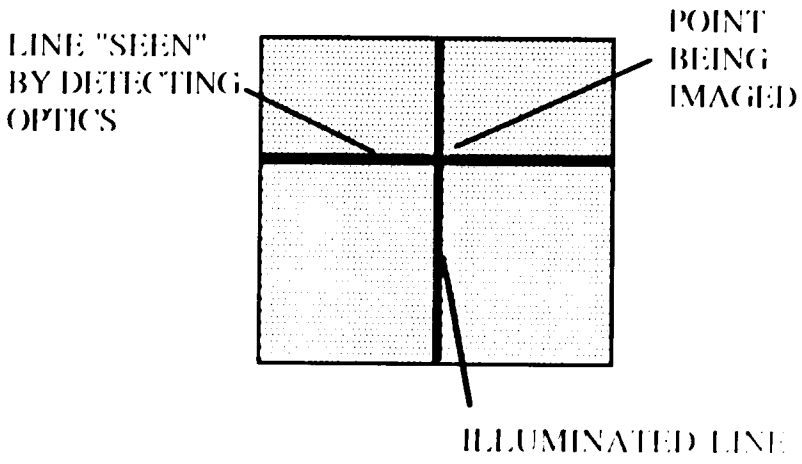


Figure 10.3. Plan View of the Specimen

surface and recording the received intensity as a function of position.

The depth of field will be large because the caustic line is relatively straight compared to its thickness so the illumination of the sample is independent of its height. The relationship between the depth of field and resolution can be calculated both for this instrument and the conventional optical microscope.

The resolution, r, is limited by the width of the Airy diffraction pattern at the caustic.

$$r^3 = \frac{\rho}{2 \cdot k^2} \tag{10.1}$$

where ρ is the radius of curvature of the caustic and k is the wavenumber. The depth of field is estimated by finding the length that can be traveled along a caustic before the transverse distortion due to the caustics curvature becomes equal to the resolution. This yields

$$\delta^2 = \frac{8 \cdot \rho}{r} \tag{10.2}$$

where δ is the depth of field.

Eliminating ρ from equations (10.1) and (10.2) yields

$$\delta = 4 \cdot kr^2 \tag{10.3}$$

For a conventional optical microscope, using coherent illumination without any coupling medium between the lens and the sample, the resolution is given by

$$r = \frac{0.61 \cdot \lambda}{\sin\theta} \tag{10.4}$$

where θ is the angle subtended at the sample by the edges of the aperture of the objective lens [BORN 1964]. Here, the depth of field is taken to be given by the height over which the rays from the object destined to reach the edge of the objective aperture spread by a distance r. These rays are diverging at an angle θ so the depth of field, δ, thus given is

$$\delta = \frac{r}{\tan\theta} \tag{10.5}$$

For small θ, the relevant approximations can be used for $\sin\theta$ and $\tan\theta$, facilitating the elimination of θ from equations (10.4) and (10.5) to yield

$$\delta = \frac{r^2}{0.61 \cdot \lambda} = \frac{r^2 k}{0.61 \cdot 2\pi} \tag{10.6}$$

For both instruments the depth of field is proportional to the square of the resolution. For any given resolution equations (10.3) and (10.6) imply that the depth of field of the caustic is greater by a factor of $0.61 \times 8\pi \simeq 15.3$.

The results of the ultrasonic experiments demonstrate that well defined caustics yielding resolutions on the order of one wavelength can be formed using reflectors on the order of wavelengths across. To reproduce these conditions optically, producing an instrument with a resolution of 1 μm would require a mirror about 25 μm which is impracticably small. As shown by equation (10.1), r increases as the cube root of the radius of the caustic implying that resolutions of about 5 μm can be achieved using mirrors with diameters of a few millimeters. In this regime

an optical microscope can be operated with θ values less than 5 degrees so the small angle approximations used in deriving equation (10.6) are justified.

Beyond the calculated depth of field the image will not be lost, as are any out of focus parts of an image formed by a conventional microscope, but distorted without any loss of clarity of detail. This means that the effective depth of field for practical purposes will be larger than that calculated above.

CHAPTER 11

DISCUSSION OF APPLICATIONS TO N.D.E.

All the research presented in the preceding chapters has possible applications. These are listed below with discussion of their advantages and disadvantages relative to conventional testing practice.

The results of the investigations in chapter 6 lead to the following method of locating relatively small defects:

A region of the rod (or pipe) under test would be illuminated with one transducer while another connected to electronics capable of recognizing the signals from a caustic would be scanned in an arc around the sample. If the angles at which caustics are found are given to a computer it can construct an image of any internal defects. This can be done very quickly because the functional dependence of the radial position of the defect on the separation of the caustics can be tabulated in the computers memory. The electronic task of recognizing caustics is by no means trivial but could be done, for example, by measuring the rate of change of amplitude of each signal inside the relevant time window.

Small defects, such as a voids and hard inclusions, can be located by this method. The criterion that the flaw should reflect sound strongly is the same as that in conventional pulse-echo testing, therefore, any ultrasonically detectable defect can be located by this method.

The resolving power of the proposed ultrasonic N.D.E technique can be estimated by considering the width of the Airy diffraction pattern around the caustic and applying Rayleigh's criterion [BORN and WOLF 1964]. This describes the ability to separately resolve two points in terms of the overlap of the diffraction patterns produced by each. The minimum distance between two small defects at which they can still be separately detected depends on the direction along which they are separated and on how near they are to the center of the sample. As an example, for 5 MHz shear waves testing a 76 mm diameter aluminum rod, the spatial resolution is 0.5 mm in the radial direction and in the circumferential direction has a linear dependence on radial position ranging from 0.5 mm at 50% of the radius to 3 mm at 90%. As the wavelength of shear sound at this frequency is 0.62 mm, the radial resolution is less than the wavelength and therefore, as good as can be achieved by any means. The resolution is not so high if the defects are close to the edge of the rod and separated along the circumferential direction. But, this is the situation in which the alternative conventional technique, focusing the sound to a point just below the surface, is most effective. Therefore, if this method is used in conjunction with ordinary focusing, defects over the full extent of the cylinder can be resolved well. Also, if short pulses of sound are being used the resolution will be increased because signals reflected from nearby points will be separated from each other by virtue of the fact that they arrive

at different times.

If these caustics are to be applied to the testing of pipes there is the extra constraint to be considered. The rays which go on to form the caustic must not hit the inner surface of the pipe. The implication of this is that there is a region of the inner part of the pipe wall that is not available for inspection by this method. The extent of this hidden zone, as a fraction of the pipe wall thickness, has been calculated for the shear wave inspection of steel. This is a function of pipe geometry as shown in figure 11.1. The percentage of the pipe that can be inspected increases as the pipe wall becomes thinner relative to its radius.

An advantage in the use of caustics to inspect pipes is that, unlike a surface breaking crack in a rod, a defect extending from the inner surface of a pipe will produce a clearly defined signal as it crosses the caustic. This allows accurate sizing of such cracks, once they extend beyond the hidden zone just described above.

A problem with this technique is that if there are N point defects in the region under inspection, 2N caustics will be formed and therefore, N(2N-1) pairs of caustics. That is, the image reconstruction algorithm will deduce 2N(N-1) "phantom" defect locations. Many of these will be disregarded because they are outside the region illuminated by the incident sound but some will confuse the image. This can be overcome by scanning the receiving transducer at two different distances from the sample and

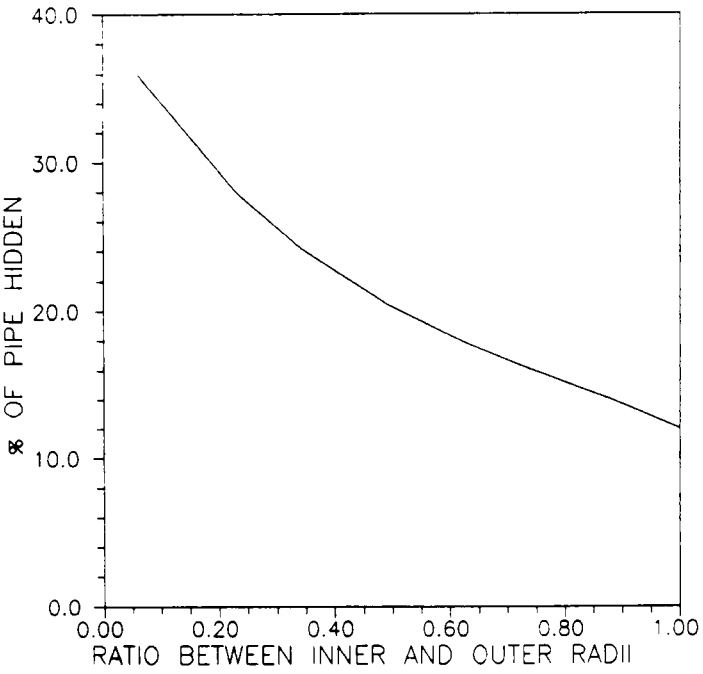


Figure 11.1. The Fraction of the Pipe Thickness Hidden as a Function of its Geometry

performing the image construction twice. The real defects will be in the same place on each image but the "phantom" image points will have moved.

An advantage of this technique is that it requires no accurate time measurements. This allows the use of long tone bursts of sound, containing a narrow frequency spectrum, rather than the usual short, broad band pulses. This of great potential value in the inspection of materials in which sound is highly dispersive in amplitude and/or velocity such as many high performance composite materials [MURRI 1989]. Not having to produce such a short pulse makes it possible to test at lower frequencies which is of help when inspecting coarse grained metals. Freedom from having to measure the time of flight could also be useful in the testing of very small components using high frequency sound where making the time measurements required for conventional pulse-echo inspection is either difficult or expensive.

Extended internal defects could be characterized by following a procedure very similar to the one described in chapter 7. An advantage of this method is that it is independent of the roughness and orientation of the crack. Conventional ultrasonic inspection is hampered by the fact that the strength of a signal from a defect depends on strongly on these two factors. The transmitter probe can be moved to any position and orientation in order to find the minimum separation between defect and the

receiver. This process leads to the elimination of all factors in the signal strength except the geometric location of the ends of the crack.

For practical application it would be beneficial if the sample could be illuminated with diffuse sound thus decreasing the dependence of the received signals on defect orientation. This could be done using several transmitters of sound each pulsing sound trough an ultrasonic diffuser, which could be any obstacle that is rough on the scale of the wavelength yet acoustically transparent.

The investigation of the shadows of surface-breaking defects showed that there is an effect due to the crack tip crossing the caustic but also geometric acoustics are quite accurately obeyed by the shadow of the defect. This implies that it is only really necessary to consider the influence of the caustic to back up the results of a conventional ultrasonic test. In cases where it is vital to know the exact nature of a crack any extra means of obtaining information is extremely valuable.

The major application of any technique capable of imaging the internal structure of an object of low acoustic refractive index is medical diagnostics. Medical ultrasonics is a large and well developed industry and many sophisticated imaging systems are on the market. Using the method described in chapter 9, scanning a caustic through the body then constructing an image from the received echoes, has the advantage that the algorithm used to form

the image is relatively simple. This means that the computer systems needed will be faster or cheaper and also more reliable.

A practical medical imaging system would involve the use of apparatus different from those used in this preliminary study. The reflecting dish forming the caustic would have to be scaled depending on the part of the body being examined and specialized point source/receiver transducers would be needed. The speed of the system could be greatly increased if, instead of scanning the caustic mechanically, an array of transducers where placed around the body and fired sequentially. It remains to be seen whether, if given the correct transducers and such electronic scanning, this technique could be developed to the point where it could compete with existing medical technology.

Any high depth of field microscope will be of great use to materials scientists, geologists and biologists. The acoustic microscope described in chapter 9 needs to be refined by placing an aperture in front of the specimen so that height profile is studied along only one thin strip of the specimen at a time. If the focusing geometry described in terms of optics in chapter 10 were to be applied to acoustics, a microscope could be made capable of producing genuine three-dimensional images of a surface. The distortion-free depth of view of such an instrument would not be limited in the same way as that of its optical

counterpart because given the time of flight of a signal the image reconstruction algorithm can account for the curvature of the caustic.

CHAPTER 12

CONCLUSIONS AND SUGGESTED FUTURE RESEARCH

The alternative approach to focusing presented in this thesis has been demonstrated to lead to novel N.D.E. techniques. The viability of the use of caustics to locate point-like and extended internal defects in rods and pipes has been shown, and use of caustics to form images has also been demonstrated. These techniques have definite advantages over conventional methods in certain situations.

A large area of future research following this project is in solving the mechanical and electrical engineering problems associated with applying this research as discussed in chapter 11. In particular, means for automatically scanning a transducer around the sample and electronics capable of recognizing signals that arise from the caustic need to be developed. In addition to this, building a workable and competitive imaging system based on the research presented in chapter 9 requires specialized ultrasonic transducer design.

The construction of a working prototype of the high depth of field microscope proposed in chapter 10 will be an interesting future project. Also, an acoustic analog of this system could be built with the capability of mapping the profile of rough surfaces in 3-dimensions.

It is concluded that the consideration of focusing phenomena in general terms, as opposed to making efforts to create point foci, has a real contribution to make to N.D.E. technology.

LIST OF REFERENCES

Abramowitz M., Stegun I.A., Hand Book of Mathematical Functions, National Bureau of Standards Applied Mathematics Series 55, Washington D.C., 1964.

Airy G.B. On the Intensity of Light in the Neighborhood of a Caustic. Trans. Cambridge. Philos. Soc., Vol. 6, 379-403 1838.

Berry M.V., Upstill, C. Catastrophe Optics: Morphologies of Caustics and Their Diffraction Patterns, in Progress in Optics (ed E. Wolf), vol XVIII, North Holland (1980) 257-346

Born M., Wolf E. Principles of optics, 3rd ed., Pergamon Press 1964

Cayley A. A Memoir Upon Caustics, Phil. Trans. Roy. Soc., Vol. 147, 273-312, 1857

Descartes R. Meteorology, 1637

Doyle P.A. Ultrasonic Caustics in Non-Destructive Evaluation, Journal of Physics D. vol 13, 163-77, 1980

Filipczynski L., Pawlowski Z., Wehr J. Ultrasonic Methods of Testing Materials, Butterworths, London 1966.

Keller J.B. Diffraction by an Aperture. Journal of Applied Physics, Vol. 28, no.4, 426-44, 1956

Krautkramer J., Krautkramer H. Ultrasonic Testing of Materials, 3rd ed., Springer-Verlag, 1983

Landau L., Lifshitz E., The Classical Theory of Fields, 1st ed, Addison-Wesley Press, Cambridge Ma., 1951.

Mason W.P., Phyical Acoustics, vols Ia to IVb, Academic Press, New York, 1968.

Moshfehgi M., Hanstead P.D. Combined Shear-Compression Ultrasound Reflection Tomography, Acoustical Imaging, vol. 14, Plenum Press, New York 1985, 425-436.

Moshfehgi, M. N.D.T. of Rods and Pipes Using Shear Wave Caustics, Ultrasonics, January 1986.

Rayleigh J.W.S.(Baron). The Theory of Sound, 2nd ed., Dover Publications, New York, 1945.

Thompson D.O. Review of Progress in Quantitative N.D.E., Plenum Press, New York 1988.

Weast R.C. **(ed.)** CRC Handbook of Chemistry and Physics, 67th ed., CRC Press, Boca Raton, Florida, 1986.

APPENDIXES

APPENDIX A

CALCULATION OF THE ORIENTATION OF THE CAUSTIC AT INFINITY

The intention is to calculate the direction in which the caustic formed by sound from a point source inside a cylinder extends to infinity. That is the direction in which neighboring rays, which are refracted out of the cylinder after one internal reflection, meet only at infinity. Referring to figure A-1, let the direction of the initial ray from the source be β and the direction of the final ray be ψ then the condition for neighboring rays to be parallel is

$$\frac{d\psi}{d\beta}=0 \tag{A-1}$$

To calculate the direction of the caustic we need to know ψ in terms of β. Consider a ray from S being reflected at A then refracted at B. From point B

$$\lambda+\theta=\gamma+\psi \tag{A-2}$$

$$\Rightarrow \psi=\lambda+\theta-\gamma \tag{A-3}$$

$$\frac{d\psi}{d\beta}=0\Rightarrow \frac{d\lambda}{d\beta}+\frac{d\theta}{d\beta}-\frac{d\gamma}{d\beta}=0 \tag{A-4}$$

Applying the sine rule to triangle ACH:

$$\frac{\sin\theta}{d}=\frac{\sin\beta}{R} \tag{A-5}$$

$$\Rightarrow \sin\theta=r\cdot\sin\beta \quad \text{where } r=\frac{d}{R} \tag{A-6}$$

$$\Rightarrow \cos\theta\cdot d\theta = r\cdot\cos\beta\cdot d\beta \tag{A-7}$$

$$\Rightarrow \frac{d\theta}{d\beta}=r\cdot\frac{\cos\beta}{\cos\theta} \tag{A-8}$$

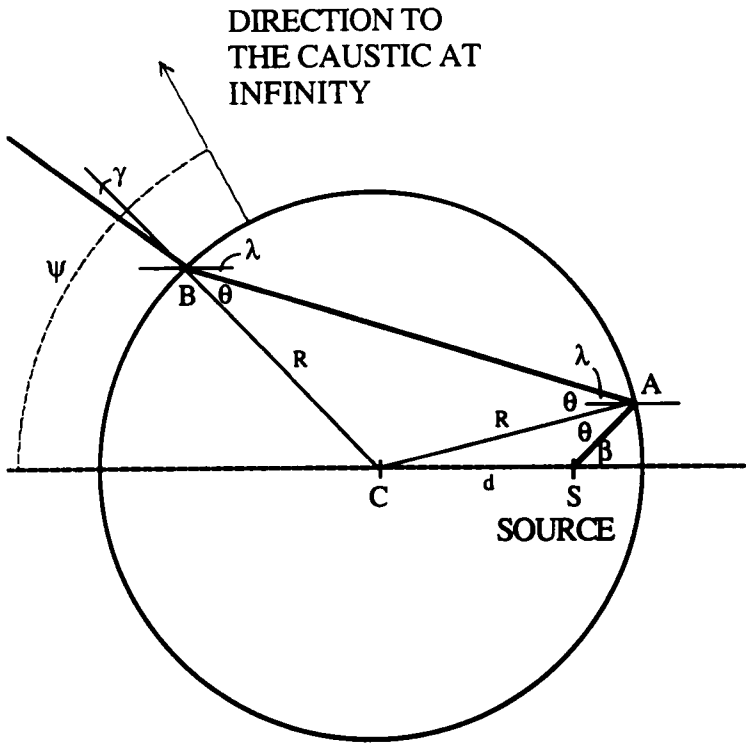


Figure A-1. The Ray Path of Sound Scattered From a Defect at S

From point A:

$$2\theta=\lambda+\beta \tag{A-9}$$

$$\Rightarrow \lambda=-\beta+2\theta \tag{A-10}$$

$$\Rightarrow \frac{d\lambda}{d\beta}=-1+2\theta \tag{A-11}$$

Applying Snell's law at B:

$$\sin\gamma=n\cdot\sin\theta \tag{A-12}$$

Where $n=\dfrac{\text{speed of sound in water}}{\text{speed of sound inside sample}}$

$$\Rightarrow \frac{d\gamma}{d\theta}=n\cdot\frac{\cos\theta}{\cos\gamma} \tag{A-13}$$

Using sin γ from (A-12):

$$\frac{d\gamma}{d\theta}=\frac{n\cdot\cos\theta}{\sqrt{1-n^2\sin^2\theta}} \tag{A-14}$$

$$\Rightarrow \frac{d\gamma}{d\beta}=\frac{d\gamma}{d\theta}\cdot\frac{d\theta}{d\beta}=\frac{d\theta}{d\beta}\cdot\frac{n\cdot\cos\theta}{\sqrt{1-n^2\sin^2\theta}} \tag{A-15}$$

Substituting $\frac{d\lambda}{d\beta}$ and $\frac{d\gamma}{d\beta}$ from (A-11) and (A-15) into (A-4)

$$\Rightarrow -1+2\cdot\frac{d\theta}{d\beta}+\frac{d\theta}{d\beta}-\frac{d\theta}{d\beta}\cdot\frac{n\cdot\cos\theta}{\sqrt{1-n^2\sin^2\theta}}=0 \tag{A-16}$$

$$\Rightarrow \frac{d\theta}{d\beta}\cdot\left[3-\frac{n\cdot\cos\theta}{\sqrt{1-n^2\sin^2\theta}}\right]-1=0 \tag{A-17}$$

From (A-8):

$$\frac{d\theta}{d\beta}=\frac{r\cdot\sqrt{1-\sin^2\beta}}{\cos\theta} \tag{A-18}$$

Substituting β from (A-6):

$$\frac{d\theta}{d\beta}=\frac{r}{\cos\theta}\cdot\sqrt{1-\frac{1}{r^2}\cdot\sin^2\theta} \tag{A-19}$$

Substituting this into equation A-17 yields an implicit equation for the critical value of θ (θ_c).

$$\frac{\sqrt{r^2-s^2}}{c}\cdot\left[3-\frac{n\cdot c}{\sqrt{1-n^2s^2}}\right]-1=0 \qquad \text{(A-20)}$$

Where: $s = \sin\theta_c$

$c = \cos\theta_c$

Substituting λ from (A-10), β from (A-8) and γ from (A-12) into (A-2) implies:

$$\psi_c=3\theta_c-\sin^{-1}(n\cdot\sin\theta_c)-\sin^{-1}\left(\frac{1}{r}\cdot\sin\theta_c\right) \qquad \text{(A-21)}$$

This gives the direction of the caustic at infinity, ψ_c, in terms of θ_c which must be obtained by solving (A-20) with the relevant values of n and r.

APPENDIX B

THE LOCUS OF THE CAUSTIC FORMED BY A CIRCULAR REFLECTOR

Referring to figure B-1, consider a point source of rays at S. After reflection at A each ray can be described by $y=M(\theta)\cdot x+C(\theta)$ where θ is the initial direction of the ray.

Applying the sine rule to triangle ACH:

$$\frac{1}{r}\cdot\sin\phi=\sin(180-\theta)=\sin\theta \qquad \text{(B-1)}$$

$$\phi=\sin^{-1}(r\cdot\sin\theta) \qquad \text{(B-2)}$$

From triangle ACH:

$$90-\beta=\theta-\phi \qquad \text{(B-3)}$$

Applying sine rule to triangle ACH:

$$\frac{1}{C}\cdot\sin\phi=\sin(180-(\beta+\phi))=\sin(\beta+\phi)=\sin(90-\theta+2\cdot\phi)=\cos(\theta-2\cdot\phi) \qquad \text{(B-4)}$$

$$C=\frac{\sin\phi}{\cos(\theta-2\cdot\phi)} \qquad \text{(B-5)}$$

From triangle ADH:

$$2\cdot\phi=\theta+180-\alpha \qquad \text{(B-6)}$$

$$\alpha=180+\theta-2\cdot\phi \qquad \text{(B-7)}$$

$$M=\tan(\alpha) \Rightarrow M=-\tan(2\cdot\phi-\theta) \qquad \text{(B-8)}$$

The equation for the reflected rays is:

$$y=-\tan(2\cdot\phi-\theta)\cdot x+\frac{\sin(\phi)}{\cos(\theta-2\cdot\phi)} \qquad \text{(B-9)}$$

The caustic is the locus of the points of intersection of neighboring rays. Consider two rays; $y=M(\theta)\cdot x+C(\theta)$ and $y=M(\theta+\Delta\theta)\cdot x+C(\theta+\Delta\theta)$ meeting at point by (X,Y).

$$M(\theta)\cdot X+C(\theta)=M(\theta+\Delta\theta)\cdot X+C(\theta+\Delta\theta) \qquad \text{(B-10)}$$

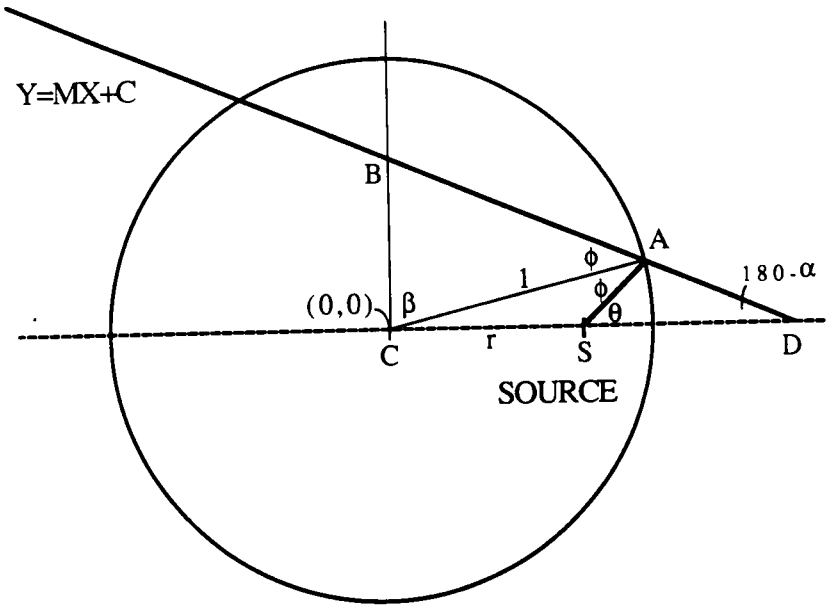


Figure B-1. Ray Reflected by a Circular Reflector

$$\Rightarrow X=\frac{(C(\theta+\Delta\theta)-C(\theta))}{(M(\theta+\Delta\theta)-C(\theta))} \tag{B-11}$$

As $\Delta\theta$ is small:

$$C(\theta+\Delta\theta)-C(\theta)=\frac{dC}{d\theta}\cdot\Delta\theta \tag{B-12}$$

$$M(\theta+\Delta\theta)-M(\theta)=\frac{dC}{d\theta}\cdot\Delta\theta \tag{B-13}$$

$$\Rightarrow X=-\frac{\frac{dC}{d\theta}}{\frac{dM}{d\theta}} \tag{B-14}$$

Differentiating C from equation B-5 with respect to θ:

$$\frac{dC}{d\theta}=\frac{\cos(\theta-2\cdot\phi)\cdot\cos\phi\cdot\phi'+\sin(\theta-2\cdot\phi)\cdot(1-2\cdot\phi')}{(\cos(\theta-2\phi))^2} \tag{B-15}$$

Where $\phi'=\frac{d\phi}{d\theta}$. Differentiating ϕ from equation (B-1):

$$\cos\phi\cdot\phi'=r\cdot\cos\theta \Rightarrow \phi'=r\cdot\frac{\cos\theta}{\cos\theta} \tag{B-16}$$

$$\frac{dC}{d\theta}=\frac{r\cdot\cos(\theta-2\cdot\phi)\cdot\cos\theta+\tan\phi\cdot\sin(\theta-2\cdot\phi)\cdot(\cos\phi-2\cdot r\cos\theta)}{(\cos(\theta-2\cdot\phi))^2} \tag{B-17}$$

$$\frac{dM}{d\theta}=\frac{d}{d\theta}\cdot(-\tan(2\cdot\phi-\theta)=\frac{-(2\cdot\phi'-1)}{\cos^2(\theta-2\cdot\phi)} \tag{B-18}$$

$$\Rightarrow \frac{dM}{d\theta}=\frac{\cos\theta-2\cdot r\cdot\cos\theta}{\cos^2(2\cdot\phi-\theta)\cdot\cos\theta} \tag{B-19}$$

Substituting (B-17) and (B-19) into (B-14):

$$X=-\frac{\{r\cdot\cos(\theta-2\cdot\phi)\cdot\cos\theta+\tan\phi\cdot\sin(\theta-2\cdot\phi)\cdot(\cos\phi-2\cdot r\cdot\cos\theta)\}\cdot\cos\phi}{\cos\phi-2\cdot r\cdot\cos\theta} \tag{B-20}$$

$$Y=M\cdot X+C \Rightarrow Y=-\tan(2\cdot\phi-\theta)\cdot X+\frac{\sin\phi}{\cos(\theta-2\cdot\phi)} \tag{B-21}$$

As ϕ is related to θ by equation (B-2), equations (B-20) and (B-21) give the locus of the caustic, (X,Y), in terms of a single parameter, θ.

VITA

James Robert Brewster was born in May 1965 in Enfield, Middlesex, Great Britain. He was brought up in Corby, Northamptonshire, an industrial town of 50,000 people in the East Midlands region of England.

He received his secondary education at Southwood Comprehensive School, Corby, obtaining advanced level certificates of education in mathematics, physics and chemistry and also passed the special examination in physics.

He attended College at the University of Bristol, England, and in 1986 graduated with a Bachelors degree in physics. While at Bristol the author worked with Dr. Ken Ashbee who, on being awarded a chair of excellence at the University of Tennessee, Knoxville, offered him the opportunity to attend graduate school in the U.S.A.. James has been in America since June 1987 and has obtained a grade point average of 3.85 for graduate courses in Materials Science, Physics and Engineering Science. He has also taught astronomy labs at U.T.K..

The author's hobbies include cycling, playing the guitar and increasing his general knowledge of science and science related issues.